



Published in final edited form as:

*ACS Biomater Sci Eng.* 2020 January 13; 6(1): 182–197. doi:10.1021/acsbomaterials.9b01496.

## Vapor-Deposited Biointerfaces and Bacteria: An Evolving Conversation

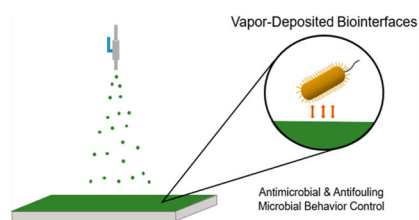
Trevor B. Donadt, Rong Yang\*

Robert F. Smith School of Chemical & Biomolecular Engineering, Cornell University, Ithaca, New York 14853, United States

### Abstract

At the biointerface where materials and microorganisms meet, the organic and synthetic worlds merge into a new science that directs the design and safe use of synthetic materials for biological applications. Vapor deposition techniques provide an effective way to control the material properties of these biointerfaces with molecular-level precision that is important for biomaterials to interface with bacteria. In recent years, biointerface research that focuses on bacteria–surface interactions has been primarily driven by the goals of killing bacteria (antimicrobial) and fouling prevention (antifouling). Nevertheless, vapor deposition techniques have the potential to create biointerfaces with features that can manipulate and dictate the behavior of bacteria rather than killing or deterring them. In this review, we focus on recent advances in antimicrobial and antifouling biointerfaces produced through vapor deposition and provide an outlook on opportunities to capitalize on the features of these techniques to find unexplored connections between surface features and microbial behavior.

### Graphical Abstract



### Keywords

biointerface; antifouling; antimicrobial; vapor deposition; CVD; PVD

\*Corresponding Author: ry295@cornell.edu.

Author Contributions

The manuscript was written through contributions of all authors. All authors have given approval to the final version of the manuscript.

The authors declare no competing financial interest.

## 1. INTRODUCTION

The term “biointerface” refers to the area of contact between biological organisms or biomolecules and another material. Surfaces at which bacteria interact physically and chemically with synthetic materials constitute an important form of biointerface, the engineering of which could find applications ranging from implantable biomaterials to wastewater treatment.<sup>1–3</sup> Although the properties of antifouling (i.e., repelling bacteria/biomolecules) and antimicrobial (i.e., killing bacteria that come into contact) have been the primary foci of bacteriacentric biointerface engineering research, recent technological advances in interface engineering are poised to push the boundaries of how surfaces interact with bacteria toward more sophisticated, intricate modes of communication.

Numerous microbial-repellant strategies have been identified for biointerfaces, including chemical moieties (e.g., zwitterionic structures analogous to the head groups of membrane lipids),<sup>4–6</sup> physical structures (e.g., nanostructures found on insect wings and plant leaves),<sup>7</sup> and bacterial signaling molecules (e.g., emergent functionalities from quorum sensing/quenching).<sup>8</sup> Coatings that have become predominant in recent years feature a multitude of mechanisms to ward off or kill bacteria.<sup>9</sup> Among antifouling materials, detailed study and application of poly(ethylene glycol) (PEG) have been complemented by a focus on zwitterionic coatings, superhydrophobic materials, and surface topology. Moreover, contact-active materials, whose antimicrobial activity stems from quaternary ammonium compounds (QACs) and antimicrobial peptides (AMPs), have been realized by anchoring these molecules to polymer brushes that are coated on a substrate.

A few of the antifouling/antimicrobial strategies have been commercialized as surface modifications for implants and other medical solutions to mitigate infections and associated medical complications.<sup>10–13</sup> Continued development of microbial centric biointerfaces has expanded applications beyond biomedical devices into environmental science (e.g., ship hull fouling resistance),<sup>14,15</sup> consumer products (e.g., antibacterial textiles for medical care or athletic clothing),<sup>16</sup> and the food industry (e.g., eradication of bacteria during the preparation of edible products)<sup>17</sup> yet maintained its focus on antimicrobial and antifouling outcomes.

Conventional solution-based coating techniques to create biointerfaces include spin coating, dip coating, spray coating, and layer-by-layer deposition (see refs 18 and 19 for a review of solution-based techniques).<sup>18,19</sup> Structural characteristics (e.g., thickness and roughness) of the resultant coatings are typically linked to the solvent rheology and the drying process inherent to each solution-based procedure.<sup>20–22</sup> This makes it challenging to independently and simultaneously define the chemistry and structure of the resulting film, which is likely required for the molecular-level engineering of next-generation biointerfaces.

Vapor-based surface modification techniques, such as chemical vapor deposition (CVD) and physical vapor deposition (PVD), provide an effective way to decouple and thus exert simultaneous control over multiple surface properties.<sup>23,24</sup> CVD primarily comprises technologies in which the reaction of vapor-phase (or aerosolized) reagents deposits a product layer onto a substrate surface. The operating pressure of CVD processes can vary

from atmospheric pressure to medium vacuum to high or ultrahigh vacuum. Often, the most intricate chemistry is performed under medium to high vacuum conditions [e.g., initiated CVD (iCVD),<sup>25–28</sup> plasma-enhanced CVD (PECVD),<sup>29–31</sup> parylene CVD,<sup>32</sup> oxidative CVD (oCVD),<sup>33–35</sup> and atomic layer deposition (ALD)<sup>36,37</sup>], in which vapor phase transport in the Knudsen diffusion regime ensures conformal coverage of the vapor-deposited coating on micro- and nanostructures. PVD comprises technologies that produce thin films similar to CVD, but without reliance on a chemically reactive species. Instead, PVD utilizes energetic means to transfer atoms, or clusters of atoms, from a liquid or solid sample through a vacuum in the vapor phase onto a substrate (see Figure 1 for details about the CVD and PVD techniques named in this review).<sup>38</sup>

Table 1 outlines the mechanistic differences among the vapor deposition techniques discussed in this review. The descriptions highlight the key components of each technique and the common experimental setups to execute those components. However, the design and utilization of each vapor deposition reactor is highly flexible and often customized. For example, substrate surfaces in PECVD may or may not be heated depending on the targeted surface properties of a biointerface. The CVD techniques share many common characteristics, but there are also important distinctions in their mechanistic features. In the cases of iCVD, PECVD, parylene CVD, and flame-assisted CVD (FACVD), the reactive precursor is commonly delivered as a volatile vapor (and heated as needed), while aerosol-assisted CVD (AACVD) relies on the dissolution of precursors in a solvent that is aerosolized using an aerosol generator.<sup>39</sup> Most CVD techniques require an energy source to kick-start the reaction that leads to deposition—the heated filament array in iCVD, plasma in PECVD, the pyrolysis furnace for parylene CVD, and the flame in FACVD—while others rely on spontaneous chemical reactions between two components, such as the chemisorption to the preceding layer in ALD and oxidation in oCVD. A complete account of these differences can be found in Table 1.

Vapor deposition methods can produce biointerfaces made of inorganic and/or organic materials. Inorganic coatings (e.g., metals and metal oxides) could be deposited through CVD or PVD, both of which could overcome the challenges associated with vaporizing inorganic raw materials. PVD often directly vaporizes the target coating material, while CVD often utilizes a metal-containing compound as a precursor and chemical reactions to convert the precursor into an inorganic coating. CVD techniques that utilize high-energy species (e.g., plasma), such as PECVD, and AACVD have been used to produce both inorganic and organic materials. Nevertheless, the CVD methods with benign reaction conditions, such as iCVD, oCVD, and parylene CVD, are designed to produce organic materials such as polymers and graphene with complete retention of chemical functionalities.

Compared to solution-based biointerface engineering techniques, vapor deposition processes benefit from a solvent-free and substrate-independent nature. When considering vapor-deposited polymer coatings as an example, the absence of solvents affords several distinct advantages: (1) some vapor techniques, such as iCVD, are compatible with delicate substrates such as paper or fabrics, allowing control of device mechanical properties (e.g., to match the elastic modulus of human tissue) independent of the device surface chemistry;<sup>40</sup>

(2) the requirement of an often-incomplete solvent removal step is eliminated, enhancing the purity of the final film and thus the biocompatibility; (3) any restrictions on polymer solubility, as often required by solution coating techniques, are eliminated.<sup>41</sup> Insoluble, cross-linked polymers can thus be synthesized and made into a coating in a single step, improving durability of the modified surface using vapor deposition techniques. The removal of solvent from the synthetic process is also crucial for generating amphiphilic biointerfaces, composed of elements with contrasting wettability that lack a common solvent. (Amphiphilic materials with precisely controlled wettability are of interest for antifouling applications because of their distinct fouling repellent mechanism.)<sup>42,43</sup>

In comparison to solution-based coating techniques, there are also aspects of vapor deposition that may be viewed as less desirable. Some techniques are limited to precursors with high volatility.<sup>44</sup> Others may require high-temperature conditions or the presence of high-energy species (like plasma),<sup>45,46</sup> which could be costly and/or damaging to the delicate substrates (i.e., ones with limited thermal or chemical resistance) used to fabricate biomaterials.<sup>47</sup> A few techniques are limited to depositing coatings in a line-of-sight manner, which obscures the underlying structures that may be important for biointerfaces.

Recent technological advances have addressed some of these limitations. Room-temperature and conformal deposition that does not require high-energy plasma has been achieved using techniques such as iCVD.<sup>48</sup> Moreover, many of the aforementioned issues could be averted simply by resorting to the flexibility in the choice of vapor deposition parameters and instrument configurations. One such example is the use of carrier gas and bubblers to deliver monomers with low volatility,<sup>49</sup> thus expanding the library of vapor-deposited chemistries. Altogether the broad range of vapor deposition techniques enables the creation of biointerfaces that consist of a large variety of materials: inorganic and organic matters, homopolymers and copolymers, nanoparticles and thin films, and much more that are reviewed below in the context of bacteria-centric applications.

The biocompatibility, access to insoluble molecules, and independent control of structure and chemistry that is characteristic of vapor deposition methods bolster their potential for creating surfaces that can interface with living systems.<sup>50</sup> Bacteria outside of a laboratory setting are most commonly found in the form of surface-attached communities called biofilms.<sup>51,52</sup> These matrix-bound structures afford advantages to the survival of microbes and can be found in nearly every environment on Earth.<sup>53</sup> Microbial sensory apparatuses (pili and fimbriae), which play a major role in the characteristics of biofilms,<sup>54</sup> operate at the micrometer to nanometer scale, requiring biointerfaces with heterogeneities of similar length scale in order to establish effective interference/ communication.<sup>55,56</sup>

When targeted toward bacteria, vapor-deposition techniques offer unique nanoscale control of patterned/gradient designs and topographical features, mechanical properties, and surface energy that can be leveraged to interface with the sensory apparatuses of bacteria.<sup>57,58</sup> Vapor-deposited inorganic biointerfaces are most commonly utilized for antimicrobial applications, because inorganic materials can damage bacterial membranes or generate toxic reactive species (see Section 2.1 for details). Vapor deposition of organic biointerfaces further enables the tuning of a wide range of surface features, including surface energy,

topography, stimuli-responsiveness, and incorporation of bioactive molecules (such as enzymes and peptides). These surface characteristics are most commonly tuned for antifouling applications, where the vapor-deposited biointerfaces can be hydrophilic or hydrophobic (see Section 3.1), or stimuli-responsive, i.e. changing shape/size in response to changes in pH or temperature (see Section 3.3), to ward off the attachment of microbes or to remove surface-attached colonies. In recent years, topography and incorporation of bioactive molecules have also been leveraged in antimicrobial applications (see Section 2.2). The wide range of chemistries available for vapor-deposited biointerfaces further enhances the potential to establish novel modes of surface-bacteria communication, such as controlled interactions at the biointerface that turn multicellular biofilms into therapeutic tools.<sup>59</sup>

This review will focus on vapor-deposited biointerfaces for antimicrobial and antifouling applications, as well as surface-bacteria communication beyond those two common objectives with a predominant focus on research in the past five years (Figure 2). We will first profile recent advances in antimicrobial biointerfaces, where chemical species that kill bacteria have been deposited. Subsequently, we will address recent advances in antifouling biointerfaces designed to repel the accumulation of biological materials. That discussion leads to an overview of emerging efforts in multifunctional materials, which combine both antimicrobial and antifouling properties in a single design. Finally, we will conclude with an outlook on the potential to capitalize on the conversation between biointerfaces and bacteria to dictate the bacterial phenotype or biofilm characteristics. We will discuss existing efforts to understand how materials communicate with bacteria at a biointerface beyond “kill or repel” and potential future directions for the evolving “dialogue” between biointerfaces and bacteria.

## 2. ANTIMICROBIAL BIOINTERFACES

Vapor-deposited antimicrobial surfaces can be roughly organized into two categories based on composition: those that contain inorganic antimicrobial agents and those that leverage organic species. Inorganic biointerfaces are known to have broad-spectrum antimicrobial activities.<sup>60</sup> Although a number of competing mechanisms have been proposed to explain the antimicrobial activity of inorganic materials, it is generally agreed upon that metals/metallic nanoparticles or the dissolution of metal ions disinfect by breaking down bacteria membranes, proteins, or DNA.<sup>61</sup> Organic biointerfaces herein include polymer-based and graphene-containing coatings that utilize antimicrobial mechanisms such as inhibitory topography (for graphene), antibiotic encapsulation/binding, and the presence of bactericidal functional groups.<sup>62</sup> Carbon nanotubes (CNTs) have also been used as antimicrobial agents.<sup>63,64</sup> Despite their ability to produce CNTs,<sup>65</sup> CVD techniques have not often been employed to produce CNTs for antimicrobial applications.<sup>66</sup>

The existing literature on vapor-deposited antimicrobial coatings suffers from large variabilities in the approaches adopted by different studies and research groups, including the microbes used, the assays employed to assess antimicrobial activities, and the assessment durations. That variability makes a direct comparison of antimicrobial efficacies among various biointerfaces challenging. To enable an objective evaluation of different studies/materials despite the disparities, we have included information on the microbe of interest

and duration of study, along with the report on efficacy. Furthermore, differences in the cellular architecture of Gram-negative and Gram-positive bacteria could have important ramifications on the effectiveness of antimicrobial treatments. For example, the outer membrane of Gram-negative bacteria presents a permeation barrier that is not shared by most Gram-positive bacteria, and the membranes of each type differ in thickness and structure, all of which could affect the penetration of antimicrobial species.<sup>67</sup> Some studies addressed that difference by testing their biointerface with at least one Gram-positive and one Gram-negative strain. In those cases, the antimicrobial biointerface is typically effective against both Gram-positive and Gram-negative bacteria, but to different degrees.

## 2.1. Inorganic Biointerfaces.

**2.1.1. Silver.**—Silver, particularly in the form of nanoparticles, is the most effective antimicrobial metal when applied as a coating.<sup>68</sup> It has broad applications in water treatment, air treatment, textiles, and medicine.<sup>69</sup> A multitude of proposed mechanisms for silver's bactericidal activity suggest that silver has a multifaceted impact on bacteria. Dissolved silver ions are suspected to damage chromosomal DNA and to be reactive toward thiol groups of proteins found in the membrane or cytoplasm, potentially leading to degradation of biomolecules critical for cellular functions (for a review of the biological activities, see ref 70).<sup>70,71</sup>

Recent work shows a heightened focus on silver nanoparticles on the order of 1–100 nm that feature a larger surface to volume ratio, enhancing the release of silver ions compared to solid silver films.<sup>71</sup> Silver nanoparticles can bind to membrane-bound proteins and damage the structural integrity of a cell membrane to hinder its normal functions. Furthermore, silver nanoparticles (particularly those below 10 nm in diameter) have been shown to penetrate the cell membranes/walls of bacteria, further damaging the membrane/wall and generating harm, including protein degradation from reactive oxygen species (ROS).<sup>70</sup>

Despite the popularity of silver in consumer products, the fate of silver and silver nanoparticles introduced into the human body is not fully understood.<sup>72,73</sup> Notwithstanding the reported gap between the bactericidal concentrations of silver ions (in the  $\mu\text{g/L}$  range) and the concentrations triggering severe mammalian toxicity (in the  $\text{mg/L}$  range),<sup>74</sup> biocompatibility is not guaranteed. The toxicity of silver to mammalian cells has been shown to rely on a variety of experimental factors, including culture medium composition during in vitro experiments<sup>75</sup> and particle size, chemistry, and concentration when in the nanoparticle form.<sup>76–78</sup>

To fabricate biointerfaces containing silver, CVD methods commonly reduce a silver precursor to form nanometer-scale silver layers/composites/nanoparticles, whereas PVD typically involves transfer and deposition of metal silver.<sup>79,80</sup> Coatings of pure silver have been employed for a range of antimicrobial applications. Micron-thick silver PVD coatings on limb prosthetics have been utilized to prevent infection until skin cells took over to fill that role.<sup>81</sup> Coated samples exposed to *Staphylococcus aureus*, *Staphylococcus epidermis*, and *Pseudomonas aeruginosa* in vitro generated a 5–8 log reduction in colony-forming unit (CFU) counts on the surface over the course of 72 h. The biocompatibility of the silver coating was demonstrated in a rabbit amputation model, where equivalent ingrowth of

fibrovascular connective tissue and host cells inside the pores of the implants was observed on silver-coated and uncoated implants over the course of six months. The silver-coated implant did not cause ulceration or thinning of the femur bone. Silver thin films consisting of droplets ranging from a few nanometers to 500 nm in diameter have been deposited onto titanium dioxide by AACVD,<sup>80</sup> which led to a 3-log reduction of *Escherichia coli* after 6 h of contact time under dark, in vitro conditions. Notably, silver coatings synthesized from conventional electroplating, PVD, and a method termed plasma immersion ion implantation and deposition (PIIID)—a combination of PVD and electrodeposition—have been compared in vivo.<sup>82</sup> While larger-than one-micron-thick coatings of each type reduced biofilm volume 48 h postimplantation, the PIIID-modified dental implant displayed greater bactericidal efficacy in humans. 57% of oral bacteria present on the devices were killed upon contacting PIIID-modified dental brackets, compared to 51% for PVD and 41% for electrodeposition.

Silver has also been employed with other compounds using vapor deposition to fabricate composite materials. Silver coatings on titanium, titanium oxide, and zirconium commonly have yielded greater antimicrobial activity than that of the metals and metal oxides alone while maintaining the physical strength.<sup>83–86</sup> Silver has also been layered with SiO<sub>x</sub> under atmospheric pressure conditions to reduce manufacturing cost<sup>87</sup> and integrated with highly smooth zirconia to improve antibacterial implant durability.<sup>88</sup>

Some of the studies presented here compared the impact of silver on bacteria versus mammalian cells.<sup>85</sup> Nevertheless, the toxicity of silver-based antimicrobial materials and interfaces would be best assessed in vivo on a large scale. Moreover, there is evidence that silver can breed bacterial resistance.<sup>72,91,92</sup> While recent studies have shown that silver has comparable antimicrobial activity to antibiotics (e.g., colloidal silver spray versus oral antibiotics for recalcitrant chronic rhinosinusitis),<sup>93</sup> concerns about drug resistance may undermine the potential for silver to supplant antibiotics during infection control and treatment.

**2.1.2. Copper.**—The successes and limitations of silver coatings have inspired research into probing the antimicrobial qualities of other metals as alternatives, such as copper. Similar to silver, copper is a Group 11 element commonly used in household products. Though the antimicrobial activity of copper is pathogen-specific, copper ions capable of traversing the cell membrane are known to produce destructive ROS.<sup>94</sup> Furthermore, the thiophilicity of aqueous copper ions is understood to be responsible for the replacement of iron in dehydratase complexes and disrupting metabolic functions.<sup>95</sup>

Copper is often used in combination with other inorganic materials, such as metals and metal oxides, to improve its antimicrobial efficacy, durability, or biocompatibility. Copper has been codeposited with silver via PVD to gain antimicrobial efficacy against a broader spectrum of bacteria, leveraging the diverse strain specificity of each metal.<sup>96</sup> Surprisingly, rather than the anticipated synergistic effect, 50 nm copper-silver coatings with more than 50% copper had reduced antimicrobial efficacy compared to pure silver. Samples with the lowest percentage of copper (below 22 wt %) prevented *E. coli* growth from reaching the exponential phase over the course of 100 h, in contrast to 7 h for a control culture as determined by OD<sub>600</sub> measurements. Interestingly, in the same report, copper was shown to

increase the dissolution rate of silver ions into a synthetic sweat solution, implying that the copper–silver combination might lead to greater antimicrobial activity than either metal individually. Joint replacement alloys have been coated with copper–titanium alloy (to leverage the biocompatibility of both materials), using various PVD methods.<sup>97</sup> The resulting surface was designed to feature increased adhesion of the coating to the implant and hardness compared to pure copper coatings. Alloy films deposited using a PVD method called dual high power impulse magnetron sputtering demonstrated the best antibacterial efficacy. Despite some initial bacterial growth in the first 24 h, 10-day in vitro exposures of *S. aureus* and *S. epidermidis* to the 122 nm-thick copper-titanium films led to a 6-log reduction of planktonic bacterial count.

Copper-doped silicon oxide (SiO<sub>x</sub>) films deposited by atmospheric pressure plasma vapor deposition have been investigated as a class of optically clear and durable antimicrobial nanocomposite coatings for medical devices.<sup>98</sup> This method eliminated toxic chemicals commonly used in alternative synthetic routes, which can leave hazardous residues that are prohibitive for medical devices. Copper-doped SiO<sub>x</sub> films reduced surface *E. coli* counts (evaluated by ATP luminescence) to 1% that of a control sample after 3 h. Nevertheless, fluorescent imaging revealed no significant difference in the growth of mammalian cells (osteoblastic mouse cells) over the course of 1 week compared to undoped SiO<sub>x</sub>, implying low cytotoxicity. The antimicrobial effect remained after 1,000 washing cycles despite the surface becoming smoother by losing copper-containing surface clusters. Tests of zinc-doped SiO<sub>x</sub> films under the same conditions did not yield the same degree of antimicrobial effect. Copper has also been embedded in a silica matrix using CVD to combat surface contamination in healthcare facilities.<sup>99</sup> Copper ions were released from nanostructured copper aggregates embedded within a 25 nm-thick silica matrix. The coating led to a 5-log reduction of viable *E. coli* and *P. aeruginosa* after 4 and 6 h, respectively, as well as a 5-log reduction of a disinfectant test strain of *S. aureus* after 6 h and a 3-log reduction of vancomycin-resistant *Enterococcus faecium* after 24 h.

Zirconium oxide has also been combined with copper in an AACVD process to capitalize on the mechanical strength and bioinertness of zirconium oxide<sup>100</sup> and bactericidal activity of copper. The composite coating was applied on silica for potential use in orthopedic implants.<sup>101</sup> The AACVD process created densely packed copper/zirconium oxide domains that were on the order of 50–75 nm in diameter. The coatings resulted in a 4.5-log decrease of viable *E. coli* and *S. aureus* in vitro, reaching surface bacterial counts below the 100 CFU detection limit after 20 and 60 min of contact time, respectively.

**2.1.3. Metal Oxides.**—Coatings of titanium dioxide<sup>102</sup> and copper/zinc oxides<sup>103,104</sup> have been fabricated using vapor deposition techniques to harness their inherent antibacterial nature (see below for details on their antibacterial mechanisms). Metal oxides have also been employed as a physical material enhancement (e.g., transparency) for copper-oxide based antimicrobial coatings.<sup>105</sup>

Titanium dioxide (TiO<sub>2</sub>) has received considerable attention for its antimicrobial photocatalytic activity.<sup>106</sup> In the presence of oxygen and water, TiO<sub>2</sub> can be activated by wavelengths in the ultraviolet (UV) range of 300–400 nm, generating ROS that are



damaging to bacteria.<sup>106,107</sup> TiO<sub>2</sub> can be synthesized by a wide range of methods—sol–gel, electrodeposition, hydrothermal, etc.<sup>108</sup> Vapor-deposited TiO<sub>2</sub> is often combined with other materials to introduce a complementary bactericidal mechanism that does not rely on UV exposure.<sup>80</sup> In a recent example, TiO<sub>2</sub> has been combined with copper using CVD to combat *S. aureus*.<sup>102</sup> Mixing 3.5 atom % copper into the TiO<sub>2</sub> coatings (>100 nm thick) produced maximal antibacterial effect after 3 h, although the precise reduction in bacterial count was not reported. Another study designed a self-cleaning surface that integrated antibacterial silver into an anatase TiO<sub>2</sub> matrix via CVD.<sup>109</sup> The embedded silver nanoparticles (spherical; 5–10 nm in diameter) provided a source of antimicrobial ions, while TiO<sub>2</sub> was photocatalytically activated to oxidize and to promote the removal of organic matters from the surface, thus renewing the antimicrobial capacity. Without UV exposure, antimicrobial tests (run for 24 h) on films of over 500 nm against *S. aureus* revealed maximal bactericide at 15% silver content (mole fraction based on EDS intensity). However, a trade-off between antimicrobial and self-cleaning capabilities was identified. With UV exposure, the self-cleaning ability of TiO<sub>2</sub> (defined by % degradation of the dye Orange G) was reduced by the addition of silver to the coating.

One issue facing the implementation of TiO<sub>2</sub> for antimicrobial applications is that the UV exposure required to activate TiO<sub>2</sub>'s photocatalytic activity is not always desirable. Indoor environments that would benefit from this technology, such as hospitals, often lack a readily accessible UV source; continuous UV exposure is simply not possible for implantable devices. That is why semiconducting graphitic-C<sub>3</sub>N<sub>4</sub> has been deposited onto TiO<sub>2</sub> nanotubes (chosen for enhanced photocatalytic activity)<sup>110</sup> to increase the wavelength required.<sup>111</sup> The graphitic species were reported to enable visible-light photocatalysis by lowering the band gap required to activate a redox reaction from 3.2 eV for anatase TiO<sub>2</sub> to 2.69 eV. The electron generated by graphitic-C<sub>3</sub>N<sub>4</sub> upon visible light radiation was believed to be passed to the TiO<sub>2</sub> to generate antibacterial ROS. In vitro experiments on TiO<sub>2</sub> nanotubes (two μm long and 150 nm in diameter) revealed a decrease in *E. coli* colonies from 72% of the number present on a control surface to 16% in visible light upon the addition of graphitic-C<sub>3</sub>N<sub>4</sub>.

Copper oxide depositions include both the CuO and the Cu<sub>2</sub>O oxidation states, each of which is understood to participate in antibacterial mechanisms. For example, one study of copper oxide nanoparticles found that Cu<sub>2</sub>O is able to inactivate fumarase enzymes, while CuO has the capability of generating ROS.<sup>112</sup> Despite its bactericidal efficacy, copper oxide is costly in comparison to other metal oxides and colored, detracting its suitability in hospitals and on the displays of electronic devices.<sup>105</sup> To address these issues, AACVD has been used to deposit a 500 nm film of gallium oxide and copper oxide. Gallium ions from gallium oxide are able to interrupt the iron metabolism of bacteria to complement copper oxide's production of ROS, and gallium oxide-containing films have the additional benefit of transparency. Transparency may be a requirement, e.g. when applied on touch screens, or a preference, e.g. in healthcare facilities where clarity signifies cleanliness. Films containing both materials led to a 4-log reduction of *E. coli* and *S. aureus* grown on the surface in the short term (over 24 h). Furthermore, an antimicrobial coating that is antireflective and transparent has been fabricated for electronic device touch screens by the simultaneous deposition of copper oxide and silica via FACVD.<sup>103</sup> In FACVD, a flame is used to break

down stable precursors prior to deposition. The silica-copper oxide silica coatings (of 50–100 nm for each layer) generated a 6-log reduction of *E. coli* viability in the short term (over 24 h) without sacrificing the optical clarity of pure silica due to the thinness of the copper oxide layer.

Recent advances in metal oxide depositions also include zinc oxide which derives its bactericidal capacity from ROS generating photochemical reactions, adsorption to and destabilization of cell walls, and the cytotoxicity of zinc ions.<sup>113</sup> Composites of zinc oxide and cyclodextrin along with the antibiotic cefepime were deposited using matrix-assisted pulse laser evaporation (MAPLE).<sup>114</sup> MAPLE involves ablating a precursors-containing frozen colloidal suspension into vapor using a pulsed laser. In vitro experiments using micron-thick coatings of the zinc oxide composite revealed a 2-log reduction of *E. coli* growth over the course of 24 h. Biocompatibility was assessed in vivo by injecting nanoparticles of the composite coating material into mice veins. The nanoparticles were found in the liver, lung, kidney, and spleen 2 days after the injection, but were cleared from the system and found only in the spleen after 10 days.

## 2.2. Organic Biointerfaces.

**2.2.1. Polymers.**—Polymers have been used in antimicrobial applications in two ways: by presenting a biocidal structure, or by releasing another antimicrobial agent in a sustained fashion.<sup>115</sup> In some vapor deposition experiments, polymers that are inherently antibacterial are made into coatings. The antimicrobial activity is often made possible by functionalizing the polymer side chains with biocidal moieties (e.g., quaternary ammonium or antimicrobial peptides). One such application witnessed a 5-log reduction of *S. aureus* and *E. coli* growth after contacting a guanidine-derived (1,1,3,3-tetramethylguanidine) polymer coating for 2 h (see Table 2 for illustrations of the macromolecules named in Sections 2–5 of this review).<sup>116</sup> The coating was deposited using atmospheric pressure plasma enhanced chemical vapor deposition (AP-PECVD). Another used iCVD to coat fabrics (i.e., nylon fibers) with nearly 200 nm of poly(dimethylaminomethylstyrene) (PDMAMS) and caused a 6-log reduction in viable *E. coli* over the course of 60 min.<sup>117</sup>

Polymer coatings have also been implemented as diffusive barriers to an antimicrobial species (e.g., metal or antibiotics) in order to realize its sustained release. By sandwiching silver metal between layers of poly(*p*-xylylene) (PPX), release of the underlying bactericidal metal was prolonged.<sup>118</sup> Coatings of 190 nm PPX on top of 1  $\mu\text{m}$  of silver entirely prohibited the growth of *E. coli* for four hours. The release rate of silver [650 pg/(cm<sup>2</sup>-min)] would correspond to three years of antimicrobial efficacy if implemented on an artificial bladder. In some systems, the diffusive barrier can be designed to be stimuli-responsive. One such design entailed a pH-responsive poly(acrylic acid) (PAAc) barrier layer deposited using plasma CVD (in combination with poly(1,7-octadiene) (POct), which promoted adhesion of PAAc and provided a secondary release barrier) to control the release of antibiotic levofloxacin from a porous silicon device.<sup>119</sup> The carboxyl groups of PAAc reversibly deprotonated in basic environments, resulting in negatively charged groups that repulsively stretched the polymer. This design was tailored to the increasing pH of an infected wound site such that antibiotics would be released through the vapor-deposited barrier in response

to an infection. At a pH of 8 versus 5, twice as much levofloxacin was found to diffuse through a barrier made of 180 nm PAAc and 263 nm POct. After 16 h of cumulative levofloxacin release at pH 8, the solution was diluted 1:10 into a *P. aeruginosa* culture and inhibited microbial growth, while the release at pH 5 was insufficiently antimicrobial.

Vapor-deposited functional polymers have also been used to immobilize antimicrobial peptides (AMPs), giving rise to an antimicrobial biointerface. These represent a promising class of abiotic-biotic materials that tend to be biocompatible, a favored feature for medical applications.<sup>120</sup> AMPs (both naturally derived and synthetic) commonly present cationic groups and depolarize or disrupt bacterial membranes as an antimicrobial mechanism.<sup>121</sup> AMPs are also known to modulate the host immune response in some cases and improve wound healing.<sup>120,122</sup> Vapor deposition enables the application of a coating to which AMPs may be added through subsequent chemical reactions. Thiol-ene click chemistry has been used to immobilize AMPs to iCVD-deposited poly-(2,4,6,8-tetravinyl-2,4,6,8-tetramethyl cyclotetrasiloxane) (PV4D4) layered onto a latex glove, which killed over 97% of *E. coli* and *S. aureus*.<sup>123</sup> Another study of a cecropin-melittin hybrid AMP showed enhanced biocidal activity and improved stability when immobilized on a CVD-generated polymer coating compared to a self-assembled monolayer (SAM).<sup>124</sup> Interestingly, analysis of the AMP structure during bactericidal activities highlighted the interactions between the cell membrane and charged AMP groups as the primary antimicrobial mechanism, rather than puncturing of the bacterial membrane.

**2.2.2. Graphene.**—The mechanical strength, flexibility, conductivity, thermal stability, and functionalizable nature of graphene and its derivatives make this material an intriguing candidate for applications that require both bactericide and biocompatibility.<sup>125</sup> Graphene oxide in particular, which is amenable to CVD, is capable of damaging bacterial membranes without harming mammalian cells when introduced at the right dosage.<sup>126</sup> To demonstrate those properties of graphene oxide, researchers treated MG-63 human osteoblast cells with graphene oxide nanoribbons fabricated using a coupled CVD-plasma treatment method.<sup>127</sup> When utilized at a concentration of 100  $\mu\text{g}/\text{mL}$ , the material exhibited no cytotoxicity or impact on expression of a gene encoding bone proteins. Meanwhile, bactericidal and biofilm formation experiments revealed a 50% decrease in viable bacterial counts for both *E. coli* (after 3 h) and *S. aureus* (after 12 h) at comparable graphene oxide concentrations.

Graphene has also offered a new approach to using topographic features to eradicate bacteria. Graphene nano spikes oriented away from a surface have been deposited using PECVD to examine their antibacterial activity.<sup>89</sup> Atomic force microscopy (AFM) and scanning electron microscopy (SEM) revealed small graphitic spikes on the order of 60–100 nm. This topography displayed significant bactericidal effects, achieving nearly 100% loss of cell viability after merely one hour of contact, which was attributed to a spike's ability to puncture bacterial cell walls. Interestingly, graphene spikes with heights ranging from 60 to 100 nm were lethal to *E. coli* and *S. epidermidis*, while exhibiting no toxicity to mammalian (mouse fibroblast) cells. That result was attributed to the difference in cell wall structure and strength. Use of this topographic strategy is intriguing, but has been explored infrequently in conjunction with vapor deposition in recent years.

### 3. ANTIFOULING BIOINTERFACES

Antifouling biointerfaces are surfaces equipped with chemistry that prevents biological matter—bacteria, proteins, and other cellular products—from attaching. In the case of bacteria, this inhibition of attachment has the added benefit of preventing the development of biofilms that rely on an initial attachment of planktonic bacteria. These bacterial communities are so ubiquitous that they constitute one of the major forms of biomass on our planet, and the issues they present are numerous.<sup>53</sup> In healthcare alone, 80% of human infections are attributed to biofilms that, once formed, require complex therapeutic procedures.<sup>128</sup> Even in the absence of bacteria, other cellular products can cause build-up of contaminants, such as the clogging of purification membrane pores.<sup>129</sup>

Numerous surface features have been found to reduce fouling, which include, but are not limited to, surface energy/ wettability, topography, and stimuli-responsiveness.<sup>130,131</sup> Each of these cases intersects with the field of vapor deposition most prominently through polymer coatings because of the endless variations and combinations of functional polymers that present any number of these antifouling mechanisms. As a result, polymers constitute the majority of vapor-deposited antifouling surfaces. Unlike antimicrobial biointerfaces, the differences between the efficacy of antifouling biointerfaces on Gram-positive versus Gram-negative bacteria have not been studied as thoroughly.

#### 3.1. Surface Energy.

Surface energy is the most common antifouling mechanism explored by vapor deposition techniques. It is frequently employed for dental<sup>132,133</sup> and purification membrane applications<sup>134,135</sup> owing to the warm and/or wet, bacteria-accommodating environment. The range of surface energies may be roughly categorized as amphiphilic, hydrophobic, and hydrophilic, each of which is capable of reducing the surface presence of bacteria, proteins, and biofilms under differing conditions. Hydrophilic and hydrophobic domains in amphiphilic coatings have been successful for antifouling applications but have not often been applied through vapor deposition in recent years.<sup>136</sup> Hydrophobic biointerfaces are traditionally known as self-cleaning (i.e., debris and bacteria that attach under ambient air conditions can be removed by water droplets rolling off the surface at a low sliding angle) rather than antifouling (i.e., inherently resistant to the attachment of bacteria) but can be fouling-resistant in the presence of oil.<sup>137</sup> For example, hydrophobic polymer PV4D4 has been deposited onto melamine sponges using iCVD which selectively absorbed oil from an *E. coli* contaminated water/oil mixture without bacteria uptake.<sup>138</sup> We will focus the following discussions on hydrophilic interfaces.

Hydrophilic polymers constitute the most common antifouling polymer category for use in aqueous environments. The ability of these macromolecules to bind water through chemical groups at a surface creates a large enthalpic penalty for replacing the water with biological molecules and bacteria.<sup>139,140</sup>

Poly(ethylene glycol) (PEG), also referred to as poly-(ethylene oxide) (PEO), and its derivatives are the most commonly utilized polymers for antifouling coatings of medical devices due to their biocompatibility and oxygen-containing repeat units (which act as a

hydrogen receptor, a feature considered characteristic of antifouling chemistry).<sup>140,141</sup> In one example, CVD enabled the preparation of amine-containing surfaces of poly(4-amino-*p*-xylylene-*co-p*-xylylene) onto which poly(ethylene glycol) methyl ether methacrylate (PEGMA) was layered.<sup>142</sup> Low attachment density of fluorescent kinesin motor protein probes was demonstrated by attachment rate measurements of microtubules. In another study, PEO deposited via iCVD rejected attachment of fluorescein isothiocyanate-labeled bovine serum albumin (FITC-BSA) across 90% of the surface versus less than 10% on silicon, amine, and hydroxyl controls.<sup>143</sup>

Unique among hydrophilic polymers are zwitterionic polymers which contain separated positive and negative charges that strongly bind a water layer to repel incoming foulants.<sup>144</sup> Chemical treatment of iCVD poly(4-vinylpyridine) has created sulfobetaine-containing zwitterionic surfaces that prevented biofouling in water purification environments.<sup>145</sup> Quartz crystal microbalance with dissipation monitoring (QCM-D) showed a 75% reduction in attached mass of bovine serum albumin (BSA) onto the zwitterionic coatings compared to a gold control substrate.

### 3.2. Surface Topography.

The effect of surface topography on fouling resistance has been investigated by changing the spatial arrangement of antifouling chemistry and exposing the resulting surfaces to bacteria. Due to the thin, conformal coatings that are a staple of vapor deposition, the generation of a topographically varied surface typically necessitates an additional patterning step or deposition atop a surface with preexisting topographical features. For example, PEG has been grafted (via a solution-phase treatment) onto a plasma polymerized and patterned allylamine (PAAm) surface.<sup>146</sup> SEM imaging confirmed that, after one hour of exposure, a negligible amount of *P. aeruginosa* attached to PEG-coated surfaces, while PAAm and glass controls had significant colonization. Furthermore, biofilm surface coverage of one-micron diameter PEG spots on glass was half that of 3–5  $\mu\text{m}$  spots, implying enhanced antifouling capability when surface energy and topography were engineered simultaneously. Although the effect of surface topography on the adhesion of mammalian and bacterial cells has been studied,<sup>147</sup> there are few recent examples that involve vapor-deposited biointerfaces. This identifies the combination of topography and vapor deposition as a potentially rich area for research in the future.

### 3.3. Stimuli-Responsive Fouling Resistance.

Polymers that change surface energy in response to environmental cues have been made into antifouling coatings. Such coatings could be used to encourage cell adhesion under one condition while promoting foulant removal under another. For example, iCVD has been used to incorporate stimuli-responsive poly(N-isopropylacrylamide) (PNIPAAm) onto titanium surfaces to prevent fouling commonly encountered in dental implants.<sup>148</sup> Following a deposition of 60 nm-thick poly(glycidyl methacrylate) (PGMA) onto titanium disks, PNIPAAm brushes were grafted via the epoxy groups afforded by the PGMA coating, enabling a thermal-responsive surface. At room temperature, approximately 90% of adhered *S. aureus* and *Porphyromonas gingivalis* was successfully rinsed away, while only ~40% of adhered bacteria could be washed away at a warmer mouth temperature. Nevertheless, at

mouth temperature, the polymer coating enabled adhesion of human adipose-derived stem cells, implying benign tissue reactions.

### 3.4. Incorporation of Bioactive Molecules.

In addition to surface energy, molecules with a variety of biological activities have been immobilized onto surfaces using vapor-deposition techniques as antifouling measures.

Antifouling surfaces can be made from antimicrobial compounds, especially naturally occurring ones, using vapor deposition. Inspired by the clinically proven antimicrobial characteristics of essential oils, 1,8-cineole (a precursor to tea tree oil) has been polymerized using PECVD as a coating for medical devices.<sup>149</sup> Although the surface was not antimicrobial, there was a notable antifouling effect. Biofilm coverage for *E. coli* and *S. aureus* measured in the 4–7% and 24% range, respectively, compared to approximately 40% and 68% coverage, respectively, on 1,7-octadiene controls after 5 days of incubating coated coupons with the corresponding bacteria.

Extracellular DNA (eDNA) has also been surface immobilized via vapor-deposited coatings.<sup>150</sup> eDNA was of interest because it was posited to regulate biofilm attachment given its abundance in the biosphere and proven effect of promoting biofilm growth. Plasma-polymerized allylamine provided a platform to covalently immobilize eDNA through carbodiimide chemistry upon drop-casting a solution containing 2 mg/mL eDNA of varying lengths extracted from salmon sperm. Rather than promotion of growth, *P. aeruginosa* biofilm surface coverage was reduced by more than 50% on all eDNA-coated surfaces compared to controls after one and four hours of exposure to static bacterial culture. These results brought into question the exact role eDNA plays in regulating the activity of bacteria. Anchoring eDNA to a surface may have produced charge-based antifouling effects, rather than the effects inhibiting the settlement of planktonic bacteria into a biofilm state. The latter have been shown in previous experiments where eDNA were mixed with planktonic cultures.<sup>151,152</sup>

## 4. MULTIFUNCTIONAL BIOINTERFACES

When presented alone, antimicrobial biointerfaces may suffer from increasing surface accumulation of dead bacteria cells and/or biomolecules over time. That accumulation diminishes the antimicrobial activities by shielding the surface-attached living microbes from the antimicrobial moieties.<sup>153</sup> Despite the resistance to bacterial adhesion, antifouling biointerfaces do not eliminate the presence of bacteria, which could cause infections and other complications in vivo. Consequently, researchers have sought to attain both features on a single biointerface. That biointerface could reduce bacterial attachment and eradicate attached bacteria simultaneously, yielding a multifaceted line of defense. Antimicrobial metals and antifouling organic coatings are often combined via vapor deposition techniques to fabricate those multifunctional biointerfaces. Among the antimicrobial metals, silver and copper are the most commonly used.

A superhydrophobic (i.e., advancing water contact angle greater than 150°) poly(dimethylsiloxane) (PDMS) polymer layer on a glass substrate has been coated with

antimicrobial copper nanoparticles in a two-step AACVD process.<sup>154</sup> In the antifouling experiments, samples of uncoated glass showed no resistance to the attachment by *E. coli* while samples containing the copper nanoparticles atop PDMS reduced adhesion by 50%. In antimicrobial experiments, the surfaces containing nanoparticles of around 3.5 nm in diameter reduced the amount of living bacteria to below the detection limit (>4 log reduction) in less than 15 min. PDMS surfaces without nanoparticles showed no significant reduction of living bacteria; hence, the nanoparticles are considered responsible for the antimicrobial activity.

In the same vein, silver nanowires atop a plastic substrate were coated with hydrophobic graphene using CVD for antifouling/antibacterial display screens.<sup>155</sup> The smooth graphene coating reduced biofouling while allowing antimicrobial silver to leach from beneath. The graphene/silver nanowire composite coating reduced the count of surface-attached colonies of *Candida albicans* by more than 50% compared to an uncoated control. The graphene coating was also found to stabilize the silver nanowires and preserve the antimicrobial activity even after ultrasonic elution, whereas silver nanowire coatings without graphene stopped being antimicrobial after 25 min of ultrasonic elution.

Silver NPs have also been sputtered onto the surface of ultrafiltration membranes, which were coated by poly(methyl methacrylate) (PMMA) using PECVD.<sup>156</sup> Despite a reduced flux of up to 50% compared to uncoated membranes (resulted from the additional permeation resistance introduced by the PMMA and silver NP layers), the coated membranes displayed no biofilm formation or planktonic growth of *Salmonella typhimurium* over the course of five hours of exposure to bacterial suspensions.

To address the simultaneous need for antifouling and antimicrobial interfaces on implantable devices, a PDMS tracheal stent was coated with poly(pentafluorophenyl methacrylate) (PPFM) using PECVD, and then layered with micropatterned metallic silver.<sup>157</sup> After 24 h of incubation with suspensions of *S. aureus* and *P. aeruginosa* in TSB medium, cell viability assays displayed 100% death of both pathogens. Furthermore, a lack of bacterial adhesion to the coated samples compared to a PMDS control was attributed to the simultaneous occurrence of a protective dissolving silver layer and the nanostructured surface.

In order to address the issue of biofilm formation on titanium-based implants, a hybrid coating of antimicrobial protein and stabilizing polymer was explored. MAPLE was utilized to deposit microspheres made of a physical mixture of poly(3-hydroxybutyric acid-co-3-hydroxyvaleric acid) [P(3HB-3HV)], PEG, and lysozyme, a naturally occurring antimicrobial enzyme secreted by the human immune system.<sup>90</sup> The resulting surface leveraged the solubility of PEG and the biodegradability of P(3HB-3HV) to control the release of antimicrobial lysozyme without disrupting mammalian cell growth. After 24 h of incubation with a bacterial suspension, a greater-than-4-log reduction in *S. aureus* and *P. aeruginosa* biofilm formation was observed.

Another study targeted to reduce bacterial adherence and proliferation on electrospun nanofiber meshes used for filtration membranes and tissue engineering.<sup>158</sup> Conformal polymer coatings of acrylic acid (PAAc), POct, 1,8-cineole (PCo), and PAAM were

introduced onto the surface of polystyrene meshes using plasma polymerization. The coated meshes were then brought into contact with a biofilm-coated agar plate for one hour. The attachment and viability of *E. coli* were examined using SEM and confocal imaging of LIVE/ DEAD-stained samples. The tests revealed differences between the penetration of bacteria into each mesh and the viability of those bacteria depending on the surface chemistry. The PAAm and POct coatings promoted cell attachment and displayed larger numbers of viable bacteria compared to uncoated samples, whereas PAAc and PCo reduced the number of attached cells (comparative viability unclear).

One distinct method known as “kill-and-release” leverages both surface chemistry and adaptive morphology to kill attached bacteria and release them in response to external stimuli. Stimuli-responsive PNIPAAm has been deposited in a hybrid layer with a quaternary ammonium salt (QAS), [(3-trimethoxysilyl)propyl]ammonium chloride, using resonant infrared matrix-assisted pulsed laser evaporation (RIR-MAPLE).<sup>159</sup> At higher temperature (37 °C), surface-attached *S. epidermidis* cells were killed upon contact with the QAS species, while at a lower temperature (25 °C), the PNIPAAm surface component promoted detachment of the dead bacteria. The switch was enabled by a change in the surface energy at around 32 °C, the lower critical solution temperature (LCST) of PNIPAAm. The hybrid coating killed approximately 80% of attached *E. coli* and *S. epidermidis* after two hours of incubation at 37 °C and released around 60% of the attached bacteria when cooled to 25 °C.

## 5. OUTLOOK: MORE SOPHISTICATED SURFACE COMMUNICATION AND INTERACTIONS

The ubiquity of biofilms across all of Earth’s environments marks them as an alluring target for applications that are beneficial to humankind. Despite the overwhelming amount of research aimed at killing or avoiding the adherence of bacteria, not all microbes are harmful. Some have the potential to be harnessed, without needing genetic modifications, for application in fields like medical care, food preparation, agriculture, and environmental health.<sup>160</sup> The bacteria within biofilms may act as biosynthetic agents to produce chemicals through fermentation or bioremediation, while some biofilm components have applications in biotechnology, such as proteins capable of stabilizing foods and cosmetics.<sup>161,162</sup> For synthetic biointerfaces to realize the goal of dictating the behavior of attached biofilm communities, research must push toward a deeper understanding of the relationship between surfaces and microbes that links material properties with the phenotype of exposed bacteria.

There is an increasing awareness that bacteria in sessile, biofilm communities exhibit drastically different behaviors compared to those associated with the planktonic state. Studies of biochemical pathways have revealed the upregulation of quorum sensing molecules, increased microbial virulence, and protection from immune system attack among bacteria in biofilms.<sup>163,164</sup> However, less is known about how surface properties trigger those responses. The growing knowledge base of how and why bacteria attach to a surface should be accompanied by insight into the relationship between surface properties (e.g., chemistry or morphology) and the resulting bacterial genotype and phenotype. Establishing



the correlation between material properties and microbial behavior is the key to enabling systematic manipulation or inhibition of biofilm characteristics with specificity.

To date, there have been a handful of studies attempting to establish the correlation between material properties and bacterial behavior. For example, surface stiffness has been revealed as a physical characteristic that may influence the activity of attached bacteria. Studies of *P. aeruginosa* and *E. coli* grown on PMDS substrates of varying stiffness revealed a decrease in antibiotic susceptibility on stiffer surfaces.<sup>165</sup> That enhanced drug resistance could be partially attributed to the observed effect of surface stiffness to alter the size of attached bacteria. After 3.5 h of exposure to ofloxacin, 8.8% of *E. coli* survived on 2.6 MPa PDMS while 3.1% did on the less stiff 0.1 MPa PDMS. Sensing of surface stiffness was later discovered to be influenced in part by the *motB* gene, which promotes adhesion on softer surfaces.<sup>166</sup>

Though relatively unexplored by vapor deposition research, topography has been shown to influence biofilm activity. Micron-scale square features were found to promote the horizontal gene transfer (i.e., conjugation) associated with antimicrobial resistance in *E. coli* biofilm communities.<sup>167</sup> That influence was exerted by generating spots of increased cell density at the vertical sides of square features that were 10  $\mu\text{m}$  in height. In another example, a hybrid chemical–topographic approach (realized by patterning alkanethiols) was used to control the degree of isolation of discrete *E. coli* clusters.<sup>168</sup> The patterned alkanethiols (squares 5–50  $\mu\text{m}$  wide and spaced 2–50  $\mu\text{m}$  apart) provided a standard attachment environment for discrete *E. coli* clusters. Measurements of the Cell Cluster Interaction Index (defined in this paper to quantify the interaction between clusters) revealed 10  $\mu\text{m}$  to be a critical distance beyond which the ability to form connections among adjacent clusters was hindered. Studies of genetic mutants of the *luxS* gene revealed that the quorum sensing molecule, autoinducer 2 (AI-2), was involved in each cluster’s sensing of the local environment and the decision-making of whether or not to form bridges between clusters.

Recently, researchers uncovered evidence that surface chemistry could affect bacterial production of specific toxins. During the concurrent treatment of *P. aeruginosa* with ciprofloxacin and DC electrical stimulation (to generate dissolved ROS), DNA microarray analysis revealed the upregulation of different toxin-producing genes when carbon or stainless steel was used as the electrode.<sup>169</sup> Eighteen phage related genes were found to be induced by the carbon electrode compared to the stainless steel electrode. Of those, 17 were associated with the production of pyocin, a stress indicating molecule.

To date, vapor deposition solutions for surface–microbial communication that evades a goal of killing or fouling prevention have been scarce. A recent study touched upon this topic, but instead of a planar biointerface, the impact of nanoparticles on biofilms was studied. In this work, sulfur-functionalized fullerene (SFF) nanoparticles were associated with the expression of exotoxin A (*toxA*, a primary virulence factor) by *P. aeruginosa*.<sup>170</sup> SSF nanoparticles synthesized via CVD resulted in a 36% reduction in *toxA* expression, potentially providing an opportunity for treatment of *P. aeruginosa* infections. Studies of this kind highlight the promise of surface characteristics as influencers on microbes. Establishing direct correlations between material properties and microbial behaviors (elicited by surface

attachment) requires precise and independent control of surface properties (like surface chemistry, morphology, structure, and mechanical strength), for which vapor deposition may be appropriate.

As vapor-deposited biointerface design advances, manipulating microbiological behavior using biomaterials could be realized by combining the advantages inherent to this technique with knowledge from fundamental microbiology. Studies on mammalian cells and how they react to surface properties could inform the biomaterials research that focus on biofilms. For example, micro- and nanopatterned structures, including nanotubes and nanoparticles, have been shown to dictate the adhesion, morphology, and other qualities of mammalian cell communities—an outcome that could inspire similar approaches to control bacterial communities.<sup>171</sup> This endeavor also presents an opportunity to address issues of long-term effectiveness in the activity of biointerfacial features on biofilm communities.<sup>172</sup> On the most fundamental level, such an endeavor allows better understanding of the interactions between synthetic materials, the modern tool used by mankind to explore and engineer their surroundings, and one of the most ubiquitous and ancient biological systems on the planet.

## ■ ACKNOWLEDGMENTS

This work was financially supported by NIHDC016644 to R.Y.

## ■ REFERENCES

- (1). Alsteens D; Gaub HE; Newton R; Pfreundschuh M; Gerber C; Müller DJ Atomic Force Microscopy-Based Characterization and Design of Biointerfaces. *Nat. Rev. Mater* 2017, 2, 17008.
- (2). Arciola CR; Campoccia D; Montanaro L Implant Infections: Adhesion, Biofilm Formation and Immune Evasion. *Nat. Rev. Microbiol* 2018, 16, 397–409. [PubMed: 29720707]
- (3). Zhang W; Li C Exploiting Quorum Sensing Interfering Strategies in Gram-Negative Bacteria for the Enhancement of Environmental Applications. *Front. Microbiol* 2016, 6, 1535. [PubMed: 26779175]
- (4). Yesilyurt V; Veisheh O; Doloff JC; Li J; Bose S; Xie X; Bader AR; Chen M; Webber MJ; Vegas AJ; Langer R; Anderson DG A Facile and Versatile Method to Endow Biomaterial Devices with Zwitterionic Surface Coatings. *Adv. Healthcare Mater* 2017, 6, 1601091.
- (5). Yang R; Jang H; Stocker R; Gleason KK Synergistic Prevention of Biofouling in Seawater Desalination by Zwitterionic Surfaces and Low-Level Chlorination. *Adv. Mater* 2014, 26, 1711–1718. [PubMed: 24375685]
- (6). Laschewsky A Structures and Synthesis of Zwitterionic Polymers. *Polymers (Basel, Switz.)* 2014, 6, 1544–1601.
- (7). Tripathy A; Sen P; Su B; Briscoe WH Natural and Bioinspired Nanostructured Bactericidal Surfaces. *Adv. Colloid Interface Sci* 2017, 248, 85–104. [PubMed: 28780961]
- (8). Grandclément C; Tannières M; Moréra S; Dessaux Y; Faure D Quorum Quenching: Role in Nature and Applied Developments. *FEMS Microbiol. Rev* 2016, 40, 86–116. [PubMed: 26432822]
- (9). Adlhart C; Verran J; Azevedo NF; Olmez H; Keinänen-Toivola MM; Gouveia I; Melo LF; Crijns F Surface Modifications for Antimicrobial Effects in the Healthcare Setting: A Critical Overview. *J. Hosp. Infect* 2018, 99, 239–249. [PubMed: 29410096]
- (10). Civantos A; Martínez-Campos E; Ramos V; Elvira C; Gallardo A; Abarrategi A Titanium Coatings and Surface Modifications: Toward Clinically Useful Bioactive Implants. *ACS Biomater. Sci. Eng* 2017, 3, 1245–1261.
- (11). Smith RS; Zhang Z; Bouchard M; Li J; Lapp HS; Brotske GR; Lucchino DL; Weaver D; Roth LA; Coury A; Biggerstaff J; Sukavaneshvar S; Langer R; Loose C Vascular Catheters with a

- Nonleaching Poly-Sulfobetaine Surface Modification Reduce Thrombus Formation and Microbial Attachment. *Sci. Transl. Med* 2012, 4, 153ra132.
- (12). Bosco R; Van Den Beucken J; Leeuwenburgh S; Jansen J Surface Engineering for Bone Implants: A Trend from Passive to Active Surfaces. *Coatings* 2012, 2, 95–119.
- (13). Silver S; Phung LT; Silver G Silver as Biocides in Burn and Wound Dressings and Bacterial Resistance to Silver Compounds. *J. Ind. Microbiol. Biotechnol* 2006, 33, 627–634. [PubMed: 16761169]
- (14). Leonardi AK; Ober CK Polymer-Based Marine Antifouling and Fouling Release Surfaces: Strategies for Synthesis and Modification. *Annu. Rev. Chem. Biomol. Eng* 2019, 10, 241–264. [PubMed: 31173523]
- (15). Selim MS; Shenashen MA; Elmarakbi A; Fathallah NA; Hasegawa S; El-Safty SA Synthesis of Ultrahydrophobic and Thermally Stable Inorganic–Organic Nanocomposites for Self-Cleaning Foul Release Coatings. *Chem. Eng. J* 2017, 320, 653–666.
- (16). Morais SD; Guedes MR; Lopes AM Antimicrobial Approaches for Textiles: From Research to Market. *Materials* 2016, 9, 498–509.
- (17). Bastarrachea LJ; Denis-Rohr A; Goddard JM Antimicrobial Food Equipment Coatings: Applications and Challenges. *Annu. Rev. Food Sci. Technol* 2015, 6, 97–118. [PubMed: 25422880]
- (18). Richardson JJ; Cui J; Björnalm M; Braunger JA; Ejima H; Caruso F Innovation in Layer-by-Layer Assembly. *Chem. Rev* 2016, 116, 14828–14867. [PubMed: 27960272]
- (19). Barroso G; Li Q; Bordia RK; Motz G Polymeric and Ceramic Silicon-Based Coatings – a Review. *J. Mater. Chem. A* 2019, 7, 1936–1963.
- (20). Eslamian M Spray-on Thin Film PV Solar Cells: Advances, Potentials and Challenges. *Coatings* 2014, 4, 60–84.
- (21). Eslamian M Inorganic and Organic Solution-Processed Thin Film Devices. *Nano-Micro Lett.* 2017, 9, 3.
- (22). Wang Q; Xie Y; Soltani-Kordshuli F; Eslamian M Progress in Emerging Solution-Processed Thin Film Solar Cells – Part I: Polymer Solar Cells. *Renewable Sustainable Energy Rev.* 2016, 56, 347–361.
- (23). Alf ME; Asatekin A; Barr MC; Baxamusa SH; Chelawat H; Ozaydin-Ince G; Petruczuk CD; Sreenivasan R; Tenhaeff WE; Trujillo NJ; Vaddiraju S; Xu J; Gleason KK Chemical Vapor Deposition of Conformal, Functional, and Responsive Polymer Films. *Adv. Mater* 2010, 22, 1993–2027. [PubMed: 20544886]
- (24). Baxamusa SH; Im SG; Gleason KK Initiated and Oxidative Chemical Vapor Deposition: A Scalable Method for Conformal and Functional Polymer Films on Real Substrates. *Phys. Chem. Chem. Phys* 2009, 11, 5227–5240. [PubMed: 19551189]
- (25). Schröder S; Strunskus T; Rehders S; Gleason KK; Faupel F Tunable Polytetrafluoroethylene Electret Films with Extraordinary Charge Stability Synthesized by Initiated Chemical Vapor Deposition for Organic Electronics Applications. *Sci. Rep* 2019, 9, 2237. [PubMed: 30783115]
- (26). Moon H; Jeong K; Kwak MJ; Choi SQ; Im SG Solvent-Free Deposition of Ultrathin Copolymer Films with Tunable Viscoelasticity for Application to Pressure-Sensitive Adhesives. *ACS Appl. Mater. Interfaces* 2018, 10, 32668–32677. [PubMed: 30175915]
- (27). Dianat G; Gupta M Sequential Deposition of Patterned Porous Polymers Using Poly(Dimethylsiloxane) Masks. *Polymer* 2017, 126, 463–469.
- (28). Muralter F; Coclite AM; Werzer O Wrinkling of an Enteric Coating Induced by Vapor-Deposited Stimuli-Responsive Hydrogel Thin Films. *J. Phys. Chem. C* 2019, 123, 24165–24171.
- (29). Stokes K; Boonen W; Geaney H; Kennedy T; Borsa D; Ryan KM Tunable Core–Shell Nanowire Active Material for High Capacity Li-Ion Battery Anodes Comprised of PECVD Deposited ASi on Directly Grown Ge Nanowires. *ACS Appl. Mater. Interfaces* 2019, 11, 19372–19380. [PubMed: 31059229]
- (30). Li M; Liu D; Wei D; Song X; Wei D; Wee ATS Controllable Synthesis of Graphene by Plasma-Enhanced Chemical Vapor Deposition and Its Related Applications. *Adv. Sci* 2016, 3, 1600003.

- (31). Mecwan MM; Taylor MJ; Graham DJ; Ratner BD Highly-Reactive Haloester Surface Initiators for ARGET ATRP Readily Prepared by Radio Frequency Glow Discharge Plasma. *Biointerphases* 2019, 14, 41006.
- (32). Fortin JB; Lu T-M In Step-by-Step Guide to Depositing Parylene BT - Chemical Vapor Deposition Polymerization: The Growth and Properties of Parylene Thin Films; Fortin JB, Lu T-M, Eds.; Springer US: Boston, MA, 2004; pp 23–26, DOI: 10.1007/978-1-4757-3901-5\_3.
- (33). Coclite AM; Howden RM; Borrelli DC; Petruczuk CD; Yang R; Yagüe JL; Ugur A; Chen N; Lee S; Jo WJ; Liu A; Wang X; Gleason KK 25th Anniversary Article: CVD Polymers: A New Paradigm for Surface Modification and Device Fabrication. *Adv. Mater* 2013, 25, 5392–5423. [PubMed: 24115244]
- (34). Smolin YY; Soroush M; Lau KKS Influence of OCVD Polyaniline Film Chemistry in Carbon-Based Supercapacitors. *Ind. Eng. Chem. Res* 2017, 56, 6221–6228.
- (35). Wang X; Zhang X; Sun L; Lee D; Lee S; Wang M; Zhao J; Shao-Horn Y; Dinc M; Palacios T; Gleason KK High Electrical Conductivity and Carrier Mobility in OCVD PEDOT Thin Films by Engineered Crystallization and Acid Treatment. *Sci. Adv* 2018, 4, eaat5780. [PubMed: 30225366]
- (36). Kääriäinen T; Cameron D; Kääriäinen M-L; Sherman A Fundamentals of Atomic Layer Deposition In Atomic Layer Deposition; Wiley Online Books; 2013; pp 1–31, DOI: 10.1002/9781118747407.ch1.
- (37). Singh JA; Thissen NFW; Kim W-H; Johnson H; Kessels WMM; Bol AA; Bent SF; Mackus AJM Area-Selective Atomic Layer Deposition of Metal Oxides on Noble Metals through Catalytic Oxygen Activation. *Chem. Mater* 2018, 30, 663–670. [PubMed: 29503508]
- (38). Rossnagel SM Thin Film Deposition with Physical Vapor Deposition and Related Technologies. *J. Vac. Sci. Technol., A* 2003, 21, S74–S87
- (39). Hou X; Choy K-L Processing and Applications of Aerosol-Assisted Chemical Vapor Deposition. *Chem. Vap. Deposition* 2006, 12, 583–596.
- (40). Soto D; Ugr A; Farnham TA; Gleason KK; Varanasi KK Short-Fluorinated ICVD Coatings for Nonwetting Fabrics. *Adv. Funct. Mater* 2018, 28, 1707355.
- (41). Gleason KK Overview of Chemically Vapor Deposited (CVD) Polymers; Wiley Online Books; 2015, DOI: 10.1002/9783527690275.ch1.
- (42). Bhalani DV; Jewrajka SK Fouling Resistant Amphiphilic Poly(Dimethylsiloxane)-Linked-Poly(Ethylene Glycol) Network on Ultrafiltration Poly(Vinylidene Fluoride) Membrane and Effect of Spatial Chain Arrangement on Separation of Oil-Water Emulsions. *J. Membr. Sci* 2019, 583, 278–291.
- (43). Choudhury RR; Gohil JM; Mohanty S; Nayak SK Antifouling, Fouling Release and Antimicrobial Materials for Surface Modification of Reverse Osmosis and Nanofiltration Membranes. *J. Mater. Chem. A* 2018, 6, 313–333.
- (44). Knapp CE; Carmalt CJ Solution Based CVD of Main Group Materials. *Chem. Soc. Rev* 2016, 45, 1036–1064. [PubMed: 26446057]
- (45). Hamedani Y In Plasma-Enhanced Chemical Vapor Deposition: Where We Are and the Outlook for the Future; Macha P, Ed.; IntechOpen: Rijeka, 2016; pp 247–280, DOI: 10.5772/64654.
- (46). Fotovvati B; Namdari N; Dehghanhadikolaei A On Coating Techniques for Surface Protection: A Review. *J. Manuf. Mater. Process* 2019, 3, 28–50.
- (47). Rogers JA Materials for Biointegrated Electronic and Microfluidic Systems. *MRS Bull.* 2019, 44, 195–202.
- (48). Yu SJ; Pak K; Kwak MJ; Joo M; Kim BJ; Oh MS; Baek J; Park H; Choi G; Kim DH; Choi J; Choi Y; Shin J; Moon H; Lee E; Im SG Initiated Chemical Vapor Deposition: A Versatile Tool for Various Device Applications. *Adv. Eng. Mater* 2018, 20, 1700622.
- (49). Maslar JE; Kimes WA; Sperling BA; Kanjolia RK Characterization of Bubbler Performance for Low-Volatility Liquid Precursor Delivery. *J. Vac. Sci. Technol., A* 2019, 37, 41506.
- (50). Ross AM; Lahann J Current Trends and Challenges in Biointerfaces Science and Engineering. *Annu. Rev. Chem. Biomol. Eng* 2015, 6, 161–186. [PubMed: 26247290]
- (51). Davey ME; O'Toole GA Microbial Biofilms: From Ecology to Molecular Genetics. *Microbiol. Mol. Biol. Rev* 2000, 64, 847–867. [PubMed: 11104821]

- (52). Stoodley P; Sauer K; Davies DG; Costerton JW Biofilms as Complex Differentiated Communities. *Annu. Rev. Microbiol* 2002, 56, 187–209. [PubMed: 12142477]
- (53). Flemming H-C; Wuertz S Bacteria and Archaea on Earth and Their Abundance in Biofilms. *Nat. Rev. Microbiol* 2019, 17, 247–260. [PubMed: 30760902]
- (54). Craig L; Forest KT; Maier B Type IV Pili: Dynamics, Biophysics and Functional Consequences. *Nat. Rev. Microbiol* 2019, 17, 429–440. [PubMed: 30988511]
- (55). Michalska M; Gambacorta F; Divan R; Aranson IS; Sokolov A; Noiro P; Laible PD Tuning Antimicrobial Properties of Biomimetic Nanopatterned Surfaces. *Nanoscale* 2018, 10, 6639–6650. [PubMed: 29582025]
- (56). Yu Q; Cho J; Shivapooja P; Ista LK; López GP Nanopatterned Smart Polymer Surfaces for Controlled Attachment, Killing, and Release of Bacteria. *ACS Appl. Mater. Interfaces* 2013, 5, 9295–9304. [PubMed: 24041191]
- (57). Koenig M; Lahann J Nanotopographical Control of Surfaces Using Chemical Vapor Deposition Processes. *Beilstein J. Nanotechnol* 2017, 8, 1250–1256. [PubMed: 28685125]
- (58). Chen H-Y Micro- and Nano-Surface Structures Based on Vapor-Deposited Polymers. *Beilstein J. Nanotechnol* 2017, 8, 1366–374. [PubMed: 28900592]
- (59). Flores-Valdez MA Vaccines Directed Against Microorganisms or Their Products Present During Biofilm Lifestyle: Can We Make a Translation as a Broad Biological Model to Tuberculosis? *Front. Microbiol* 2016, 7, 14. [PubMed: 26834732]
- (60). Turner RJ Metal-Based Antimicrobial Strategies. *Microb. Biotechnol* 2017, 10, 1062–1065. [PubMed: 28745454]
- (61). Slavin YN; Asnis J; Häfeli UO; Bach H Metal Nanoparticles: Understanding the Mechanisms behind Antibacterial Activity. *J. Nanobiotechnol* 2017, 15, 65.
- (62). Baghdachi J; Xu Q Antibacterial Polymers and Coatings In Functional Polymer Coatings; Wiley Online Books: 2015; pp 280–295, DOI: 10.1002/9781118883051.ch10.
- (63). Al-Jumaili A; Alancherry S; Bazaka K; Jacob VM Review on the Antimicrobial Properties of Carbon Nanostructures. *Materials* 2017, 10, 1066.
- (64). Mocan T; Matea CT; Pop T; Mosteanu O; Buzoianu AD; Suci S; Puia C; Zdrehus C; Iancu C; Mocan L Carbon Nanotubes as Anti-Bacterial Agents. *Cell. Mol. Life Sci* 2017, 74, 3467–3479. [PubMed: 28536787]
- (65). Manawi MY; Ihsanullah Samara, A.; Al-Ansari T; Atieh AM A Review of Carbon Nanomaterials' Synthesis via the Chemical Vapor Deposition (CVD) Method. *Materials* 2018, 11, 822.
- (66). Akhavan O; Abdollah M; Abdi Y; Mohajerzadeh S Silver Nanoparticles within Vertically Aligned Multi-Wall Carbon Nanotubes with Open Tips for Antibacterial Purposes. *J. Mater. Chem* 2011, 21, 387–393.
- (67). Li J; Koh J-J; Liu S; Lakshminarayanan R; Verma CS; Beuerman RW Membrane Active Antimicrobial Peptides: Translating Mechanistic Insights to Design. *Front. Neurosci* 2017, 11, 73. [PubMed: 28261050]
- (68). Paladini F; Pollini M; Sannino A; Ambrosio L Metal-Based Antibacterial Substrates for Biomedical Applications. *Biomacromolecules* 2015, 16, 1873–1885. [PubMed: 26082968]
- (69). Deshmukh SP; Patil SM; Mullani SB; Delekar SD Silver Nanoparticles as an Effective Disinfectant: A Review. *Mater. Sci. Eng., C* 2019, 97, 954–965.
- (70). Franci G; Falanga A; Galdiero S; Palomba L; Rai M; Morelli G; Galdiero M Silver Nanoparticles as Potential Antibacterial Agents. *Molecules* 2015, 20, 8856–8874. [PubMed: 25993417]
- (71). Liao C; Li Y; Tjong CS Bactericidal and Cytotoxic Properties of Silver Nanoparticles. *Int. J. Mol. Sci* 2019, 20, 449.
- (72). Marambio-Jones C; Hoek EMV A Review of the Antibacterial Effects of Silver Nanomaterials and Potential Implications for Human Health and the Environment. *J. Nanopart. Res* 2010, 12, 1531–1551.
- (73). Sim W; Barnard TR; Blaskovich MAT; Ziora MZ Antimicrobial Silver in Medicinal and Consumer Applications: A Patent Review of the Past Decade (2007–2017). *Antibiotics* 2018, 7, 93.

- (74). Piszczek P Silver Nanoparticles Fabricated Using Chemical Vapor Deposition and Atomic Layer Deposition Techniques: Properties, Applications and Perspectives: Review; Bristow ARE-MSSE-AD, Ed.; IntechOpen: Rijeka, 2018; pp 187–213, DOI: 10.5772/intechopen.71571.
- (75). Souter P; Cunningham JC; Horner A; Genever PG The Variable Toxicity of Silver Ions in Cell Culture Media. *Toxicol. In Vitro* 2019, 60, 154–159. [PubMed: 31132479]
- (76). Guo X; Li Y; Yan J; Ingle T; Jones MY; Mei N; Boudreau MD; Cunningham CK; Abbas M; Paredes AM; Zhou T; Moore MM; Howard PC; Chen T Size- and Coating-Dependent Cytotoxicity and Genotoxicity of Silver Nanoparticles Evaluated Using in Vitro Standard Assays. *Nanotoxicology* 2016, 10, 1373–1384. [PubMed: 27441588]
- (77). Ivask A; Visnapuu M; Vallotton P; Marzouk ER; Lombi E; Voelcker NH Quantitative Multimodal Analyses of Silver Nanoparticle-Cell Interactions: Implications for Cytotoxicity. *Nano- Impact* 2016, 1, 29–38.
- (78). Zhang H; Wang X; Wang M; Li L; Chang CH; Ji Z; Xia T; Nel AE Mammalian Cells Exhibit a Range of Sensitivities to Silver Nanoparticles That Are Partially Explicable by Variations in Antioxidant Defense and Metallothionein Expression. *Small* 2015, 11, 3797–3805. [PubMed: 25930061]
- (79). Perrenot P; Pairis S; Bourgault D; Caillault N Sulphur Corrosion Effect on the Electrical Performance of Silver Films Elaborated by Physical Vapor Deposition. *Vacuum* 2019, 163, 26–30.
- (80). Ponja SD; Sehmi SK; Allan E; MacRobert AJ; Parkin IP; Carmalt CJ Enhanced Bactericidal Activity of Silver Thin Films Deposited via Aerosol-Assisted Chemical Vapor Deposition. *ACS Appl. Mater. Interfaces* 2015, 7, 28616–28623. [PubMed: 26632854]
- (81). Shevtsov MA; Yudintceva NM; Blinova MI; Voronkina IV; Suslov DN; Galibin OV; Gavrillov DV; Akkaoui M; Raykhtsaum G; Albul AV; Pitkin E; Pitkin M Evaluation of the Temporary Effect of Physical Vapor Deposition Silver Coating on Resistance to Infection in Transdermal Skin and Bone Integrated Pylon with Deep Porosity. *J. Biomed. Mater. Res., Part B* 2019, 107, 169–177.
- (82). Meyer-Kobbe V; Doll K; Stiesch M; Schwestka-Polly R; Demling A Comparison of Intraoral Biofilm Reduction on Silver-Coated and Silver Ion-Implanted Stainless Steel Bracket Material. *J. Orofac. Orthop./Fortschritte der Kieferorthopädie* 2019, 80, 32–43. [PubMed: 30535568]
- (83). Unosson E; Rodriguez D; Welch K; Engqvist H Reactive Combinatorial Synthesis and Characterization of a Gradient Ag–Ti Oxide Thin Film with Antibacterial Properties. *Acta Biomater.* 2015, 11, 503–510. [PubMed: 25281786]
- (84). Kang B-M; Lim Y-S; Jeong W-J; Kang B-W; Ahn H-G Antibacterial Properties of TiAgN and ZrAgN Thin Film Coated by Physical Vapor Deposition for Medical Applications. *Trans. Electr. Electron. Mater* 2014, 15, 275–278.
- (85). Ewald A; Glückermann SK; Thull R; Gbureck U Antimicrobial Titanium/Silver PVD Coatings on Titanium. *Biomed. Eng. Online* 2006, 5, 22. [PubMed: 16556327]
- (86). Maury F; Mungkalasiri J; Bedel L; Emieux F; Dore J; Renaud FNR Comparative Study of Antibacterial Efficiency of M TiO<sub>2</sub> (M = Ag, Cu) Thin Films Grown by CVD. *Key Eng. Mater* 2014, 617, 127–130.
- (87). Zimmermann R; Pfuch A; Horn K; Weisser J; Heft A; Röder M; Linke R; Schnabelrauch M; Schimanski A An Approach to Create Silver Containing Antibacterial Coatings by Use of Atmospheric Pressure Plasma Chemical Vapour Deposition (APCVD) and Combustion Chemical Vapour Deposition (CCVD) in an Economic Way. *Plasma Processes Polym.* 2011, 8, 295–304.
- (88). Pradhaban G; Kaliaraj GS; Vishwakarma V Antibacterial Effects of Silver–Zirconia Composite Coatings Using Pulsed Laser Deposition onto 316L SS for Bio Implants. *Prog. Biomater* 2014, 3, 123–130. [PubMed: 29470770]
- (89). Pandit S; Cao Z; Mokkaleti VRSS; Celauro E; Yurgens A; Lovmar M; Westerlund F; Sun J; Mijakovic I Vertically Aligned Graphene Coating Is Bactericidal and Prevents the Formation of Bacterial Biofilms. *Adv. Mater. Interfaces* 2018, 5, 1701331.
- (90). Grumezescu V; Holban AM; Sima LE; Chiritoiu MB; Chiritoiu GN; Grumezescu AM; Ivan L; Safciuc F; Antohe F; Florica C; Luculescu CR; Chifiriuc MC; Socol G Laser Deposition of Poly(3-Hydroxybutyric Acid-Co-3-Hydroxyvaleric Acid) – Lysozyme Microspheres Based

Coatings with Anti-Microbial Properties. *Int. J. Pharm* 2017, 521, 184–195. [PubMed: 28188877]

- (91). Percival SL; Bowler PG; Russell D Bacterial Resistance to Silver in Wound Care. *J. Hosp. Infect* 2005, 60, 1–7. [PubMed: 15823649]
- (92). Silver S Bacterial Silver Resistance: Molecular Biology and Uses and Misuses of Silver Compounds. *FEMS Microbiol. Rev* 2003, 27, 341–353. [PubMed: 12829274]
- (93). Ooi ML; Richter K; Bennett C; Macias-Valle L; Vreugde S; Psaltis AJ; Wormald P-J Topical Colloidal Silver for the Treatment of Recalcitrant Chronic Rhinosinusitis. *Front. Microbiol* 2018, 9, 720. [PubMed: 29696011]
- (94). Grass G; Rensing C; Solioz M Metallic Copper as an Antimicrobial Surface. *Appl. Environ. Microbiol* 2011, 77, 1541–1547. [PubMed: 21193661]
- (95). Chaturvedi K; Henderson J Pathogenic Adaptations to Host- Derived Antibacterial Copper. *Front. Cell. Infect. Microbiol* 2014, 4, 3. [PubMed: 24551598]
- (96). Gotzmann G; Jorsch C; Wetzel C; Funk HWR Antimicrobial Effects and Dissolution Properties of Silver Copper Mixed Layers. *Surf. Coat. Technol* 2018, 336, 22–28.
- (97). Stranak V; Wulff H; Rebl H; Zietz C; Arndt K; Bogdanowicz R; Nebe B; Bader R; Podbielski A; Hubicka Z; Hippler R Deposition of Thin Titanium–Copper Films with Antimicrobial Effect by Advanced Magnetron Sputtering Methods. *Mater. Sci. Eng., C* 2011, 31, 1512–1519.
- (98). Jäger E; Schmidt J; Pfuch A; Spange S; Beier O; Jäger N; Jantschner O; Daniel R; Mitterer C Antibacterial Silicon Oxide Thin Films Doped with Zinc and Copper Grown by Atmospheric Pressure Plasma Chemical Vapor Deposition. *Nanomaterials* 2019, 9, 255.
- (99). Varghese S; Elfakhri SO; Sheel DW; Sheel P; Bolton FJE; Foster HA Antimicrobial Activity of Novel Nanostructured Cu-SiO<sub>2</sub> Coatings Prepared by Chemical Vapour Deposition against Hospital Related Pathogens. *AMB Express* 2013, 3, 53. [PubMed: 24007899]
- (100). Jayakumar R; Ramachandran R; Sudheesh Kumar PT; Divyarani VV; Srinivasan S; Chennazhi KP; Tamura H; Nair SV Fabrication of Chitin–Chitosan/Nano ZrO<sub>2</sub> Composite Scaffolds for Tissue Engineering Applications. *Int. J. Biol. Macromol* 2011, 49, 274–280. [PubMed: 21575656]
- (101). Alotaibi AM; Sathasivam S; Nair SP; Parkin IP Antibacterial Properties of Cu–ZrO<sub>2</sub> Thin Films Prepared via Aerosol Assisted Chemical Vapour Deposition. *J. Mater. Chem. B* 2016, 4, 666–671. [PubMed: 32262948]
- (102). Mungkalasiri J; Bedel L; Emieux F; Cara AV-D; Freney J; Maury F; Renaud FNR Antibacterial Properties of TiO<sub>2</sub>–Cu Composite Thin Films Grown by a One Step DLICVD Process. *Surf. Coat. Technol* 2014, 242, 187–194.
- (103). Yates HM; Sheel P; Hodgkinson JL; Warwick MEA; Elfakhri SO; Foster HA Dual Functionality Anti-Reflection and Biocidal Coatings. *Surf. Coat. Technol* 2017, 324, 201–207.
- (104). Puvvada RU; Wooding JP; Bellavia MC; McGuinness EK; Sulchek TA; Losego MD Bacterial Growth and Death on Cotton Fabrics Conformally Coated with ZnO Thin Films of Varying Thicknesses via Atomic Layer Deposition (ALD). *JOM* 2019, 71, 178–184.
- (105). Hassan IA; Sathasivam S; Islam H-U; Nair SP; Carmalt CJ Ga<sub>2</sub>O<sub>3</sub>–Cu<sub>2</sub>O: Synthesis, Characterisation and Antibacterial Properties. *RSC Adv.* 2017, 7, 551–558.
- (106). López de Dicastillo C; Patiño C; Galotto JM; Palma LJ; Alburquenque D; Escrig J Novel Antimicrobial Titanium Dioxide Nanotubes Obtained through a Combination of Atomic Layer Deposition and Electrospinning Technologies. *Nanomaterials* 2018, 8, 128.
- (107). Jia L; Huang X; Liang H; Tao Q Enhanced Hydrophilic and Antibacterial Efficiencies by the Synergetic Effect TiO<sub>2</sub> Nanofiber and Graphene Oxide in Cellulose Acetate Nanofibers. *Int. J. Biol. Macromol* 2019, 132, 1039–1043. [PubMed: 30926506]
- (108). Chen X; Mao SS Titanium Dioxide Nanomaterials: Synthesis, Properties, Modifications, and Applications. *Chem. Rev* 2007, 107, 2891–2959. [PubMed: 17590053]
- (109). Mungkalasiri J; Bedel L; Emieux F; Do e J; Renaud FNR; Sarantopoulos C; Maury F CVD Elaboration of Nanostructured TiO<sub>2</sub>-Ag Thin Films with Efficient Antibacterial Properties. *Chem. Vap. Deposition* 2010, 16, 35–41.

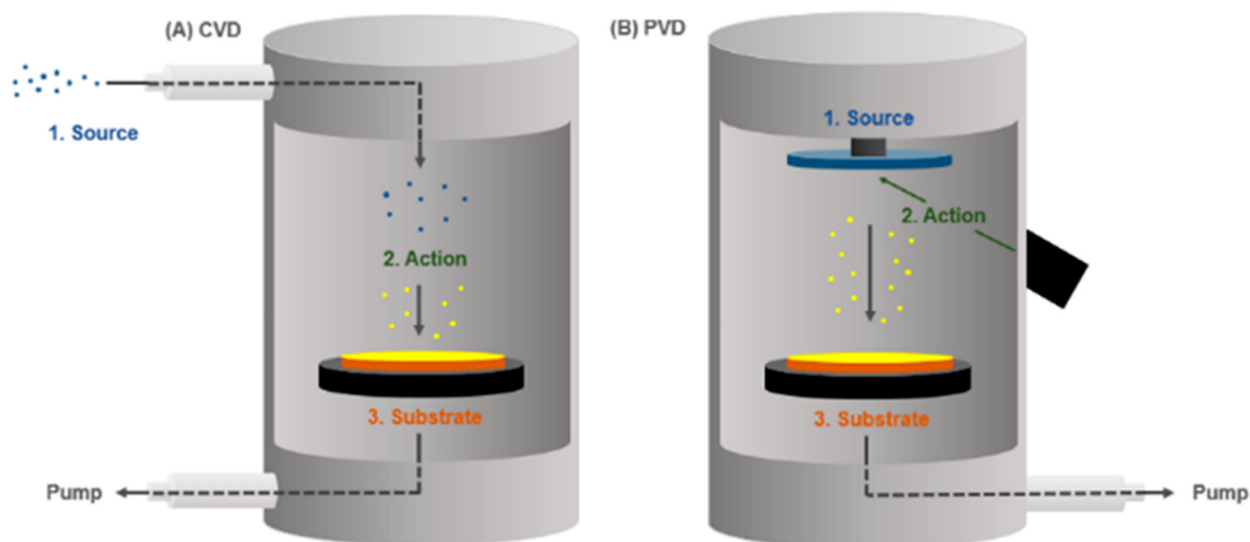
- (110). Song Y-Y; Schmidt-Stein F; Bauer S; Schmuki P Amphiphilic TiO<sub>2</sub> Nanotube Arrays: An Actively Controllable Drug Delivery System. *J. Am. Chem. Soc* 2009, 131, 4230–4232. [PubMed: 19317500]
- (111). Xu J; Li Y; Zhou X; Li Y; Gao Z-D; Song Y-Y; Schmuki P Graphitic C<sub>3</sub>N<sub>4</sub>-Sensitized TiO<sub>2</sub> Nanotube Layers: A Visible-Light Activated Efficient Metal-Free Antimicrobial Platform. *Chem. - Eur. J* 2016, 22, 3947–3951. [PubMed: 26789421]
- (112). Meghana S; Kabra P; Chakraborty S; Padmavathy N Understanding the Pathway of Antibacterial Activity of Copper Oxide Nanoparticles. *RSC Adv.* 2015, 5, 12293–12299.
- (113). Pasquet J; Chevalier Y; Couval E; Bouvier D; Bolzinger M-A Zinc Oxide as a New Antimicrobial Preservative of Topical Products: Interactions with Common Formulation Ingredients. *Int. J. Pharm* 2015, 479, 88–95. [PubMed: 25527211]
- (114). Oprea EA; Pandel ML; Dumitrescu MA; Andronescu E; Grumezescu V; Chifiriuc CM; Mogoant L; Bleanu T-A; Mogosanu DG; Socol G; Grumezescu MA; Iordache F; Maniu H; Chirea M; Holban MA Bioactive ZnO Coatings Deposited by MAPLE—An Appropriate Strategy to Produce Efficient Anti-Biofilm Surfaces. *Molecules* 2016, 21, 220.
- (115). Huang K-S; Yang C-H; Huang S-L; Chen C-Y; Lu Y-Y; Lin Y-S Recent Advances in Antimicrobial Polymers: A Mini-Review. *Int. J. Mol. Sci* 2016, 17, 1578.
- (116). Yim JH; Fleischman MS; Rodriguez-Santiago V; Piehler LT; Williams AA; Leadore JL; Pappas DD Development of Antimicrobial Coatings by Atmospheric Pressure Plasma Using a Guanidine-Based Precursor. *ACS Appl. Mater. Interfaces* 2013, 5, 11836–11843. [PubMed: 24164174]
- (117). Martin TP; Kooi SE; Chang SH; Sedransk KL; Gleason KK Initiated Chemical Vapor Deposition of Antimicrobial Polymer Coatings. *Biomaterials* 2007, 28, 909–915. [PubMed: 17095086]
- (118). Heidari Zare H; Sudhop S; Schamberger F; Franz G Microbiological Investigation of an Antibacterial Sandwich Layer System. *Biointerphases* 2014, 9, 31002.
- (119). Vasani RB; Szili EJ; Rajeev G; Voelcker NH On-Demand Antimicrobial Treatment with Antibiotic-Loaded Porous Silicon Capped with a PH-Responsive Dual Plasma Polymer Barrier. *Chem. - Asian J* 2017, 12, 1605–1614. [PubMed: 28508517]
- (120). Riool M; de Breij A; Drijfhout JW; Nibbering PH; Zaat SA J. Antimicrobial Peptides in Biomedical Device Manufacturing. *Front. Chem* 2017, 5, 63. [PubMed: 28971093]
- (121). Pasupuleti M; Schmidtchen A; Malmsten M Antimicrobial Peptides: Key Components of the Innate Immune System. *Crit. Rev. Biotechnol* 2012, 32, 143–171. [PubMed: 22074402]
- (122). Nakatsuji T; Gallo RL Antimicrobial Peptides: Old Molecules with New Ideas. *J. Invest. Dermatol* 2012, 132, 887–895. [PubMed: 22158560]
- (123). Jeong GM; Seong H; Im SG; Sung BH; Kim SC; Jeong KJ Coating of an Antimicrobial Peptide on Solid Substrate via Initiated Chemical Vapor Deposition. *J. Ind. Eng. Chem* 2018, 58, 51–56.
- (124). Xiao M; Jasensky J; Gerszberg J; Chen J; Tian J; Lin T; Lu T; Lahann J; Chen Z Chemically Immobilized Antimicrobial Peptide on Polymer and Self-Assembled Monolayer Substrates. *Langmuir* 2018, 34, 12889–12896. [PubMed: 30277782]
- (125). Han W; Wu Z; Li Y; Wang Y Graphene Family Nanomaterials (GFNs)—Promising Materials for Antimicrobial Coating and Film: A Review. *Chem. Eng. J* 2019, 358, 1022–1037.
- (126). Liao C; Li Y; Tjong CS Graphene Nanomaterials: Synthesis, Biocompatibility, and Cytotoxicity. *Int. J. Mol. Sci* 2018, 19, 3564.
- (127). Ricci R; Leite NCS; Da-Silva NS; Pacheco-Soares C; Canevari RA; Marciano FR; Webster TJ; Lobo AO Graphene Oxide Nanoribbons as Nanomaterial for Bone Regeneration: Effects on Cytotoxicity, Gene Expression and Bactericidal Effect. *Mater. Sci. Eng., C* 2017, 78, 341–348.
- (128). Mihailescu IN; Bociaga D; Socol G; Stan GE; Chifiriuc M-C; Bleotu C; Husanu MA; Popescu-Pelin G; Duta L; Luculescu CR; Negut I; Hapenciuc C; Besleaga C; Zgura I; Miculescu F Fabrication of Antimicrobial Silver-Doped Carbon Structures by Combinatorial Pulsed Laser Deposition. *Int. J. Pharm* 2016, 515, 592–606. [PubMed: 27773854]
- (129). Chen L-Y; Zhang P; Gai J-G Dendritic Molecules Give Excellent Long-Lasting Desalination Fouling Resistance to Reverse Osmosis Membrane by Generating an Amine-Rich Layer. *J. Appl. Polym. Sci* 2019, 136, 47368.



- (130). Song F; Koo H; Ren D Effects of Material Properties on Bacterial Adhesion and Biofilm Formation. *J. Dent. Res* 2015, 94, 1027–1034. [PubMed: 26001706]
- (131). Cheng Y; Feng G; Moraru CI Micro- and Nano topography Sensitive Bacterial Attachment Mechanisms: A Review. *Front. Microbiol* 2019, 10, 191. [PubMed: 30846973]
- (132). Mandracci P; Mussano F; Ceruti P; Pirri CF; Carossa S Reduction of Bacterial Adhesion on Dental Composite Resins by Silicon–Oxygen Thin Film Coatings. *Biomed. Mater* 2015, 10, 15017.
- (133). Tupinambá RA; Claro C. A. de A.; Pereira CA; Nobrega CJP; Claro APRA Bacterial Adhesion on Conventional and Self-Ligating Metallic Brackets after Surface Treatment with Plasma-Polymerized Hexamethyldisiloxane. *Dental Press J. Orthod* 2017, 22, 77–85.
- (134). Matin A; Khan Z; Gleason KK; Khaled M; Zaidi SMJ; Khalil A; Moni P; Yang R Surface-Modified Reverse Osmosis Membranes Applying a Copolymer Film to Reduce Adhesion of Bacteria as a Strategy for Biofouling Control. *Sep. Purif. Technol* 2014, 124, 117–123.
- (135). Shafi HZ; Khan Z; Yang R; Gleason KK Surface Modification of Reverse Osmosis Membranes with Zwitterionic Coating for Improved Resistance to Fouling. *Desalination* 2015, 362, 93–103.
- (136). Galli G; Martinelli E Amphiphilic Polymer Platforms: Surface Engineering of Films for Marine Antibiofouling. *Macromol. Rapid Commun* 2017, 38, 1600704.
- (137). Das S; Kumar S; Samal SK; Mohanty S; Nayak SK A Review on Superhydrophobic Polymer Nanocoatings: Recent Development and Applications. *Ind. Eng. Chem. Res* 2018, 57, 2727–2745.
- (138). Choi Y; Kim YT; You JB; Jo SH; Lee SJ; Im SG; Lee KG An Efficient Isolation of Foodborne Pathogen Using Surface-Modified Porous Sponge. *Food Chem.* 2019, 270, 445–451. [PubMed: 30174070]
- (139). Liu L; Li W; Liu Q Recent Development of Antifouling Polymers: Structure, Evaluation, and Biomedical Applications in Nano/Micro-Structures. *Wiley Interdiscip. Rev. Nanomedicine Nano biotechnology* 2014, 6, 599–614.
- (140). Damodaran VB; Murthy NS Bio-Inspired Strategies for Designing Antifouling Biomaterials. *Biomater. Res* 2016, 20, 18. [PubMed: 27326371]
- (141). Wu C; Zhou Y; Wang H; Hu J; Wang X Formation of Antifouling Functional Coating from Deposition of a Zwitterionic- Co-Nonionic Polymer via “Grafting to” Approach. *J. Saudi Chem. Soc* 2019, DOI: 10.1016/j.jscs.2019.05.011.
- (142). Katira P; Agarwal A; Fischer T; Chen H-Y; Jiang X; Lahann J; Hess H Quantifying the Performance of Protein-Resisting Surfaces at Ultra-Low Protein Coverages Using Kinesin Motor Proteins as Probes. *Adv. Mater* 2007, 19, 3171–3176.
- (143). Bose RK; Nejati S; Stuffle DR; Lau KKS Graft Polymerization of Anti-Fouling PEO Surfaces by Liquid-Free Initiated Chemical Vapor Deposition. *Macromolecules* 2012, 45, 6915–6922.
- (144). Zhang Y; Liu Y; Ren B; Zhang D; Xie S; Chang Y; Yang J; Wu J; Xu L; Zheng J Fundamentals and Applications of Zwitterionic Antifouling Polymers. *J. Phys. D: Appl. Phys* 2019, 52, 403001.
- (145). Yang R; Goktekin E; Gleason KK Zwitterionic Antifouling Coatings for the Purification of High-Salinity Shale Gas Produced Water. *Langmuir* 2015, 31, 11895–11903. [PubMed: 26449686]
- (146). Pingle H; Wang P-Y; Thissen H; McArthur S; Kingshott P Colloidal Crystal Based Plasma Polymer Patterning to Control *Pseudomonas Aeruginosa* Attachment to Surfaces. *Biointerphases* 2015, 10, 04A309.
- (147). Erramilli S; Genzer J Influence of Surface Topography Attributes on Settlement and Adhesion of Natural and Synthetic Species. *Soft Matter* 2019, 15, 4045–4067. [PubMed: 31066434]
- (148). Lee SJ; Heo DN; Lee HR; Lee D; Yu SJ; Park SA; Ko W-K; Park SW; Im SG; Moon J-H; Kwon IK Biofunctionalized Titanium with Anti-Fouling Resistance by Grafting Thermo-Responsive Polymer Brushes for the Prevention of Peri-Implantitis. *J. Mater. Chem. B* 2015, 3, 5161–5165. [PubMed: 32262590]
- (149). Mann MN; Fisher ER Investigation of Antibacterial 1,8-Cineole-Derived Thin Films Formed via Plasma-Enhanced Chemical Vapor Deposition. *ACS Appl. Mater. Interfaces* 2017, 9, 36548–36560. [PubMed: 28984443]

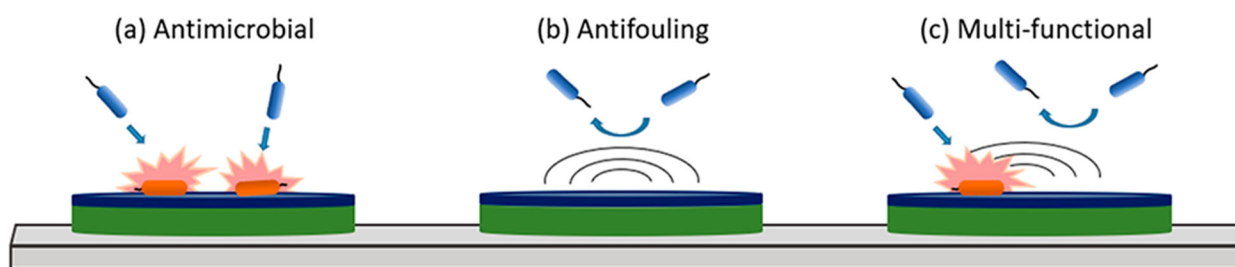
- (150). Pingle H; Wang P-Y; Cavaliere R; Whitchurch CB; Thissen H; Kingshott P Minimal Attachment of *Pseudomonas Aeruginosa* to DNA Modified Surfaces. *Biointerphases* 2018, 13, 06E405.
- (151). Harmsen M; Lappann M; Knöchel S; Molin S Role of Extracellular DNA during Biofilm Formation by *Listeria Monocytogenes*. *Appl. Environ. Microbiol* 2010, 76, 2271–2279. [PubMed: 20139319]
- (152). Berne C; Kysela DT; Brun YV A Bacterial Extracellular DNA Inhibits Settling of Motile Progeny Cells within a Biofilm. *Mol. Microbiol* 2010, 77, 815–829. [PubMed: 20598083]
- (153). Zander ZK; Becker ML Antimicrobial and Antifouling Strategies for Polymeric Medical Devices. *ACS Macro Lett.* 2018, 7, 16–25.
- (154). Ozkan E; Crick CC; Taylor A; Allan E; Parkin IP Copper-Based Water Repellent and Antibacterial Coatings by Aerosol Assisted Chemical Vapour Deposition. *Chem. Sci* 2016, 7, 5126–5131. [PubMed: 30155163]
- (155). Zhao C; Deng B; Chen G; Lei B; Hua H; Peng H; Yan Z Large-Area Chemical Vapor Deposition-Grown Monolayer Graphene-Wrapped Silver Nanowires for Broad-Spectrum and Robust Antimicrobial Coating. *Nano Res.* 2016, 9, 963–973.
- (156). Cruz MC; Ruano G; Wolf M; Hecker D; Vidaurre EC; Schmittgens R; Rajal VB Plasma Deposition of Silver Nanoparticles on Ultrafiltration Membranes: Antibacterial and Anti-Biofouling Properties. *Chem. Eng. Res. Des. Trans. Inst. Chem. Eng* 2015, 94, 524–537.
- (157). Gilabert-Porres J; Martí S; Calatayud L; Ramos V; Rosell A; Borros S Design of a Nanostructured Active Surface against Gram-Positive and Gram-Negative Bacteria through Plasma Activation and in Situ Silver Reduction. *ACS Appl. Mater. Interfaces* 2016, 8, 64–73. [PubMed: 26593038]
- (158). Abrigo M; Kingshott P; McArthur SL Bacterial Response to Different Surface Chemistries Fabricated by Plasma Polymerization on Electrospun Nanofibers. *Biointerphases* 2015, 10, 04A301.
- (159). Yu Q; Ge W; Atewologun A; López GP; Stiff-Roberts AD RIR-MAPLE Deposition of Multifunctional Films Combining Biocidal and Fouling Release Properties. *J. Mater. Chem. B* 2014, 2, 4371–4378. [PubMed: 32261577]
- (160). Tshikantwa TS; Ullah MW; He F; Yang G Current Trends and Potential Applications of Microbial Interactions for Human Welfare. *Front. Microbiol* 2018, 9, 1156. [PubMed: 29910788]
- (161). Berlanga M; Guerrero R Living Together in Biofilms: The Microbial Cell Factory and Its Biotechnological Implications. *Microb. Cell Fact* 2016, 15, 165. [PubMed: 27716327]
- (162). Jagmann N; Philipp B Design of Synthetic Microbial Communities for Biotechnological Production Processes. *J. Biotechnol* 2014, 184, 209–218. [PubMed: 24943116]
- (163). Siryaporn A; Kuchma SL; O’Toole GA; Gitai Z Surface Attachment Induces *Pseudomonas Aeruginosa* Virulence. *Proc. Natl. Acad. Sci. U. S. A* 2014, 111, 16860–16865. [PubMed: 25385640]
- (164). Tuson HH; Weibel DB Bacteria–Surface Interactions. *Soft Matter* 2013, 9, 4368–4380. [PubMed: 23930134]
- (165). Song F; Ren D Stiffness of Cross-Linked Poly-(Dimethylsiloxane) Affects Bacterial Adhesion and Antibiotic Susceptibility of Attached Cells. *Langmuir* 2014, 30, 10354–10362. [PubMed: 25117376]
- (166). Song F; Brasch ME; Wang H; Henderson JH; Sauer K; Ren D How Bacteria Respond to Material Stiffness during Attachment: A Role of *Escherichia Coli* Flagellar Motility. *ACS Appl. Mater. Interfaces* 2017, 9, 22176–22184. [PubMed: 28636823]
- (167). Gu H; Kolewe KW; Ren D Conjugation in *Escherichia Coli* Biofilms on Poly(Dimethylsiloxane) Surfaces with Microtopographic Patterns. *Langmuir* 2017, 33, 3142–3150. [PubMed: 28253620]
- (168). Gu H; Hou S; Yongyat C; De Tore S; Ren D Patterned Biofilm Formation Reveals a Mechanism for Structural Heterogeneity in Bacterial Biofilms. *Langmuir* 2013, 29, 11145–11153. [PubMed: 23919925]

- (169). Niepa THR; Snepenger LM; Wang H; Sivan S; Gilbert JL; Jones MB; Ren D Sensitizing *Pseudomonas Aeruginosa* to Antibiotics by Electrochemical Disruption of Membrane Functions. *Biomaterials* 2016, 74, 267–279. [PubMed: 26461119]
- (170). Darabpour E; Doroodmand MM; Halabian R; Imani Fooladi AA Sulfur-Functionalized Fullerene Nanoparticle as an Inhibitor and Eliminator Agent on *Pseudomonas Aeruginosa* Biofilm and Expression of ToxA Gene. *Microb. Drug Resist* 2019, 25, 594–602. [PubMed: 30461338]
- (171). Wang S; Li J; Zhou Z; Zhou S; Hu Z Micro-/Nano- Scales Direct Cell Behavior on Biomaterial Surfaces. *Molecules* 2019, 24, 75.
- (172). Hwang GB; Page K; Patir A; Nair SP; Allan E; Parkin IP The Anti-Biofouling Properties of Superhydrophobic Surfaces Are Short-Lived. *ACS Nano* 2018, 12, 6050–6058. [PubMed: 29792802]



**Figure 1.**

Generic diagrams of (A) chemical vapor deposition (CVD) and (B) physical vapor deposition (PVD). The details of the multitude of CVD and PVD processes which differentiate one technique from another are elaborated upon in Table 1. Briefly, the process characteristics can be categorized into “Source”, “Action”, and “Substrate”. Source: The precursors or reagents necessary for the deposition are unique to each technique. CVD generally applies energy to turn the precursors into vapor, which is then metered into the reactor. PVD precursors are often placed inside of the reactor. Action: In CVD, the action encompasses the reactive mechanism by which the precursors or reagents are chemically altered in preparation for deposition onto a substrate. It typically entails an energetic source and/or chemical reaction between two materials. In PVD, the action is the mechanism by which the precursors or reagents are vaporized. It typically entails an energetic input such as plasma or a laser directed at the source. Substrate: The substrate conditions differ among vapor deposition techniques, as some require a temperature-controlled or rotating substrate, or one to be placed upon an electrode. The above diagram is a conceptual representation of these steps; the configuration of reactor components and location of steps 1–3 may vary widely from process to process and diverge from the above concept. See Table 1 for an elaboration of steps 1–3 for the CVD and PVD techniques named in this review.



**Figure 2.** Vapor-deposited biointerfaces that are highlighted in this review and their interactions with microorganisms. (a) Antimicrobial interfaces kill bacteria that make contact with or come close to the surface (see Section 2); (b) antifouling interfaces reduce bacteria attachment but may not have an effect on their viability (see Section 3); (c) in this review, multifunctional interfaces refer to surfaces that display both antifouling and antimicrobial behavior (see Section 4).

Table 1.

Details of the CVD and PVD Techniques Referenced in This Review<sup>a</sup>

	(1) Source	(2) Source	(3) Source
Initiated Chemical Vapor Deposition (iCVD)	Chemical Vapor Deposition Volatile monomer and polymerization initiator	Heated filament array	Substrate cooling via temperature-controlled stage
Plasma-Enhanced Chemical Vapor Deposition (PECVD); Plasma Polymerization, & Atmospheric Pressure PECVD	Monomer vaporized by heat, as needed Volatile precursor Precursor vaporized by heat, as needed	Initiator pyrolyzed to generate free radical Plasma generated by radio frequency potential between electrodes Precursors activated to generate free radicals	Precursor adsorption promoted by cooling and polymerization upon initiator radical contact Substrate Polymerization between reactive species coats substrate
Parylene Chemical Vapor Deposition	Parylene dimer Precursor vaporized by heat	Pyrolysis furnace Dimer pyrolyzed to generate monomers	Substrate maintained at controlled temperature Polymerization on substrate
Oxidative Chemical Vapor Deposition (oCVD)	Volatile monomer precursor and oxidant Monomer and oxidant vaporized by heat, as needed	Oxidation reaction Precursor activated by reacting with oxidant	Substrate on temperature-controlled stage Monomer adsorption promoted by cooling and polymerization upon oxidant contact
Atomic Layer Deposition (ALD)	Volatile precursors Precursors vaporized by heat, as needed	Reaction between sequentially introduced precursors Vapor precursor immobilized on the surface by reacting with the surface functional group	Chemically functionalized substrate Deposition of precursors in a layer-by-layer fashion
Aerosol-Assisted Chemical Vapor Deposition (AACVD)	Nonvolatile precursor dissolved in solvent	Aerosol generator and heated zone Precursor solution aerosolized to allow transport to the substrate and solvent evaporation	Substrate heating Precursor decomposition and reaction forms coating
Flame-Assisted Chemical Vapor Deposition (FACVD)	Volatile precursors and gaseous fuel Precursors vaporized by heat, as needed, and mixed with fuel at reactor inlet	Flame generated by burning gaseous fuel Precursor fragmented by flame	Substrate heating Recombination of fragmented precursors to form a coating
Plasma Immersion Ion Implantation and Deposition (PIIID)	Solid metal precursor Precursor may be heated to promote ionization	Physical Vapor Deposition High-voltage potential pulses Ions released from precursor into vapor phase	Substrate directly facing the ion flux Recombination of ions to form a metal coating
Magnetron Sputtering	Solid metal precursor	Electrodes and magnetic field Ions freed from the metal target by inert gas plasma, which is generated by electrodes and focused by magnetic field	Substrate placed at electrode Recombination of ions to form a metal coating
Matrix-Assisted Pulsed Laser Evaporation (MAPLE)	Precursor contained in a frozen emulsion	Laser directed at frozen target	Temperature-controlled substrate directly facing the target

Author Manuscript

Author Manuscript

Author Manuscript

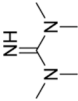
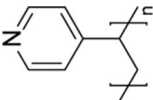
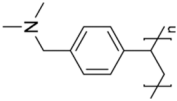
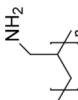
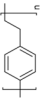
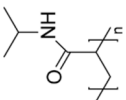
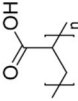
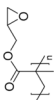

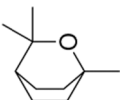
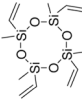
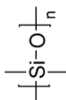

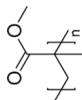
Author Manuscript

**(3) Source***Condensation of precursors***(2) Source***Precursor released by laser ablation of solvent***(1) Source**

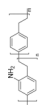
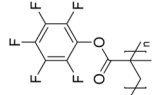
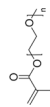
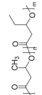
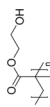
<sup>a</sup>This table contains the characteristics of each CVD/PVD technique, categorized as the "Source", "Action", and "Substrate" (same as those labeled in Figure 1). In the Source, Action, and Substrate columns, standard text describes the components present, while text in italics describes the phenomenon that occurs in that step. The table captures characteristic features for each technique; however, the precise execution/configuration may vary slightly from one research lab to another.

Table 2.

Macromolecules or Monomers Discussed in Sections 2–5 of This Review, Listed in the Order in Which They Are Mentioned

Polymer/Monomer	Acronym	Molecular Structure	Polymer/Monomer	Acronym	Molecular Structure
1,1,1,3,3 -tetramethylguanidine ( <i>monomer</i> )	-		poly(4-vinylpyridine)	P4VP	
poly(dimethylaminomethylstyrene)	PDMAMS		poly(N-allylamine)	PAAm	
poly(p-xylylene)	PPX		poly(N-isopropylacrylamide)	PNIPAAm	
poly(acrylic acid)	PAAc		poly(glycidyl methacrylate)	PGMA	
1,7-octadiene ( <i>monomer</i> )	Oct		1,8-cineole ( <i>monomer</i> )	Co	
2,4,6,8-tetravinyl-2,4,6,8-tetramethyl cyclotetrasiloxane ( <i>monomer</i> )	V4D4		poly(dimethylsiloxane)	PDMS	
poly(ethylene glycol), poly(ethylene oxide)	PEG, PEO		poly(methyl methacrylate)	PMMA	



Polymer/Monomer	Acronym	Molecular Structure	Polymer/Monomer	Acronym	Molecular Structure
poly(4-amino- <i>p</i> -xylylene- <i>co-p</i> -xylylene)	-		poly(pentafluorophenyl methacrylate)	PPFM	
poly(ethylene glycol) methyl ether methacrylate	PEGMA		poly(3-hydroxybutyric acid-co-3-hydroxyvaleric acid)	P(3HB-3HV)	
poly(2-hydroxyethyl methacrylate)	PHEMA		polystyrene	PS	